

# REPORT DOCUMENTATION PAGE

AFRL-SR-BL-TR-98-

0250

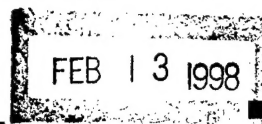
Public reporting burden for this collection of information is estimated to average 1 hour per response, including gathering and maintaining the data needed, and completing and reviewing the collection of information. Send collection of information, including suggestions for reducing this burden, to Washington Headquarters Service, Davis Highway, Suite 1204, Arlington, VA 22202-4302, and to the Office of Management and Budget, Paperwork Reduction Project (0705-0188).

1. AGENCY USE ONLY (Leave Blank)		2. REPORT DATE February 1998		3. REPORT TYPE AND DATES COVERED Final Report 03/15/94 - 12/31/97	
4. TITLE AND SUBTITLE Processing-Microstructure-Property Relationships in Advanced Intermetallics				5. FUNDING NUMBERS F49620-94-C-0023	
6. AUTHOR(S) D.A. Hardwick and P.L. Martin					
7. PERFORMING ORGANIZATION NAME(S) AND ADDRESS(ES) Rockwell Science Center, LLC P.O. Box 1085 1049 Camino Dos Rios Thousand Oaks, CA 91360				8. PERFORMING ORGANIZATION REPORT NUMBER SC71098.FR	
9. SPONSORING / MONITORING AGENCY NAME(S) AND ADDRESS(ES) AFOSR/NA Directorate of Aerospace and Materials Science 110 Duncan Ave. Bolling AFB, DC 20332-0001				10. SPONSORING / MONITORING AGENCY REPORT NUMBER Final Technical Report 0002AA	
11. SUPPLEMENTARY NOTES <i>unlimited</i>					
12a. DISTRIBUTING/AVAILABILITY STATEMENT Approved for public release; distribution is unlimited				A	
13. ABSTRACT (Maximum 200 Words) Microstructural evolution in near- $\gamma$ TiAl alloys during hot working is a complex interaction involving solid state diffusion, dynamic recrystallization and non-uniform strain accommodation. Compression workability testing, coupled with extensive metallographic characterization, has been used to study the evolution of microstructural refinement and chemical homogeneity in three near- $\gamma$ TiAl alloys: Ti-46Al-0.2B, Ti-48Al-0.2B and Ti-48Al-2Mo-0.2B. Hot working of materials that had undergone an homogenization heat treatment resulted in the breakup of the initial fully lamellar microstructures into isolated islands of lamellae surrounded by fine bands of dynamically recrystallized grains. Using material that had been initially forged to a strain of 0.9 at 1150°C with a strain rate of $10^{-3} \text{ sec}^{-1}$ , the effect of additional thermal and mechanical working steps was examined. Particular attention was paid to the effect of strain path on the behavior of the remnant lamellar colonies. Strain in the same direction as the first forging had little effect in breaking-up lamellar colonies lying in the plane of the forging while strain applied perpendicular to this direction was more effective in encouraging these features to undergo enough strain to recrystallize.					
14. SUBJECT TERMS $\gamma$ TiAl alloys, homogenization, hot workability, forging				15. NUMBER OF PAGES 36	
				16. PRICE CODE	
17. SECURITY CLASSIFICATION OF REPORT UNCLASSIFIED		18. SECURITY CLASSIFICATION OF THIS PAGE UNCLASSIFIED		19. SECURITY CLASSIFICATION OF ABSTRACT UNCLASSIFIED	
20. LIMITATION OF ABSTRACT None					

19980317 093

DTIC QUALITY INSPECTED

# Processing-Microstructure-Property Relationships in Advanced Intermetallics



## Final Technical Report

Contract No. F49620-94-C-0023

Contract period: 03/15/94 - 12/31/97

### Research Contributors:

Dr. Dallis A. Hardwick and Dr. Patrick L. Martin  
Rockwell Science Center  
1049 Camino Dos Rios  
Thousand Oaks, CA 91360

February 1998



Science Center

Copy # 1

**REPORT DOCUMENTATION PAGE**Form Approved  
OMB No. 0704-0188

Public reporting burden for this collection of information is estimated to average 1 hour per response, including the time for reviewing instructions, searching existing data sources, gathering and maintaining the data needed, and completing and reviewing the collection of information. Send comments regarding this burden estimate or any other aspect of this collection of information, including suggestions for reducing this burden, to Washington Headquarters Services, Directorate for Information Operations and Reports, 1215 Jefferson Davis Highway, Suite 1204, Arlington, VA. 22202-4302, and to the Office of Management and Budget, Paperwork Reduction Project (0704-0188), Washington, DC 20503

1. AGENCY USE ONLY (Leave Blank)		2. REPORT DATE <b>February 1998</b>	3. REPORT TYPE AND DATES COVERED <b>Final Report 03/15/94 - 12/31/97</b>	
4. TITLE AND SUBTITLE <b>Processing-Microstructure-Property Relationships in Advanced Intermetallics</b>			5. FUNDING NUMBERS <b>F49620-94-C-0023</b>	
6. AUTHOR(S) <b>D.A. Hardwick and P.L. Martin</b>				
7. PERFORMING ORGANIZATION NAME(S) AND ADDRESS(ES) <b>Rockwell Science Center, LLC P.O. Box 1085 1049 Camino Dos Rios Thousand Oaks, CA 91360</b>			8. PERFORMING ORGANIZATION REPORT NUMBER <b>SC71098.FR</b>	
9. SPONSORING / MONITORING AGENCY NAME(S) AND ADDRESS(ES) <b>AFOSR/NA Directorate of Aerospace and Materials Science 110 Duncan Ave. Bolling AFB, DC 20332-0001</b>			10. SPONSORING / MONITORING AGENCY REPORT NUMBER <b>Final Technical Report 0002AA</b>	
11. SUPPLEMENTARY NOTES				
12a. DISTRIBUTING/AVAILABILITY STATEMENT <b>Approved for public release; distribution is unlimited</b>			12b. DISTRIBUTION CODE <b>A</b>	
13. ABSTRACT (Maximum 200 Words) Microstructural evolution in near- $\gamma$ TiAl alloys during hot working is a complex interaction involving solid state diffusion, dynamic recrystallization and non-uniform strain accommodation. Compression workability testing, coupled with extensive metallographic characterization, has been used to study the evolution of microstructural refinement and chemical homogeneity in three near- $\gamma$ TiAl alloys: Ti-46Al-0.2B, Ti-48Al-0.2B and Ti-48Al-2Mo-0.2B. Hot working of materials that had undergone an homogenization heat treatment resulted in the breakup of the initial fully lamellar microstructures into isolated islands of lamellae surrounded by fine bands of dynamically recrystallized grains. Using material that had been initially forged to a strain of 0.9 at 1150°C with a strain rate of $10^{-3} \text{ sec}^{-1}$ , the effect of additional thermal and mechanical working steps was examined. Particular attention was paid to the effect of strain path on the behavior of the remnant lamellar colonies. Strain in the same direction as the first forging had little effect in breaking-up lamellar colonies lying in the plane of the forging while strain applied perpendicular to this direction was more effective in encouraging these features to undergo enough strain to recrystallize.				
14. SUBJECT TERMS <b><math>\gamma</math> TiAl alloys, homogenization, hot workability, forging</b>			15. NUMBER OF PAGES <b>36</b>	
			16. PRICE CODE	
17. SECURITY CLASSIFICATION OF REPORT <b>UNCLASSIFIED</b>	18. SECURITY CLASSIFICATION OF THIS PAGE <b>UNCLASSIFIED</b>	19. SECURITY CLASSIFICATION OF ABSTRACT <b>UNCLASSIFIED</b>	20. LIMITATION OF ABSTRACT <b>None</b>	

# **Processing-Microstructure-Property Relationships in Advanced Intermetallics**

**Contract Number: F49620-94-C-0023**

## **Final Technical Report**

**Contract Period: March 15, 1994 through December 31, 1997**

### **Research Contributors:**

Dr Dallis A. Hardwick and Dr Patrick L. Martin  
*Rockwell Science Center,  
1049 Camino Dos Rios,  
Thousand Oaks. CA 91360.*



## Executive Summary

### Objective:

The objective of this research was to define an optimum path for attaining a uniform fine grain size in the intermetallic alloy  $\gamma$ -TiAl. This was accomplished by developing an understanding of the microstructural evolution during hot working and subsequent static recrystallization. Hot workability testing allowed us to establish a quantitative framework for the selection of thermomechanical processing parameters based on the optimization of strain rate sensitivity. Ultimately, this will lead to the development of innovative thermomechanical processing techniques that will facilitate control of the chemical homogeneity and the microstructure in multi-component intermetallic alloys such as  $\gamma$ -TiAl.

### Approach:

Starting with ingot material, workability testing at a range of temperatures and strain rates was used at each step of a multi-step processing sequence to assess the material. This information, in conjunction with microstructural characterization, was used to determine the exact processing parameters of temperature and strain rate for the next processing operation. Once the processing is understood based on this iterative approach, a processing route incorporating continuous changes in strain rate and temperature could be designed and used to produce  $\gamma$ -TiAl with a refined, submicron grain size.

### Publications Resulting from this Work

D.A. Hardwick and P.L. Martin: "Mechanistic Study of Hot Working of a Cast Multi-Phase Near- $\gamma$  TiAl Alloy", Proceedings of the 35th Annual Conference of Metallurgists, (Canadian Institute of Metallurgy, 1996).

D.A. Hardwick and P.L. Martin: "A Mechanistic Study of Hot Working of Cast Gamma TiAl", in Advances in the Science and Technology of Titanium Alloy Processing, edited by I. Weiss, R. Srinivasan, P. Bania and D. Eylon, TMS, (1996) pp 153-160.

M. De Graef, D.A. Hardwick and P.L. Martin: "Structural Evolution of Titanium Diborides in Wrought Ti-47at%Al-2at%Mo-0.2at%B", in Structural Intermetallics 1997, edited by M.V. Nathal et al., TMS, (1997) pp 185-193.

D. A. Hardwick: "A Mechanistic Study of Multi-step Working in Gamma TiAl Alloys", in Thermec '97, edited by T. Chandra and T. Sakai, TMS (1997) pp 1481-1488.

## Introduction

A consensus has begun to develop in the aerospace industry that the  $\gamma$ -TiAl-base alloys could replace heavier nickel-base alloys in some applications (1, 2). Although many concerns remain, recent results indicate that gamma-TiAl has sufficient ductility to survive normal manufacturing, assembly and engine operations (3, 4).

$\gamma$ -TiAl has been plagued by limited room temperature ductility but recently, ductility has been shown to be maximized in binary alloys with an Al content around 48at% (5, 6). The Al content of gamma alloys of most interest for future applications fall in the range 45-48 at% Al. As shown in the binary phase diagram, Figure 1, this composition range straddles both the peritectic composition of 46.5 at% and the eutectoid reaction. The chemical inhomogeneities and microstructures generated by these phase transitions must be reckoned with in cast materials. Furthermore, the development of TiAl alloys has reached the stage where the addition of refractory elements, at the 1-4at% level, is quite common (7). Such additions exacerbate the problems of segregation as they diffuse more slowly than either Ti or Al. The elimination of segregation in these alloys through hot working has been, and continues to be, a subject receiving considerable attention (8-10).

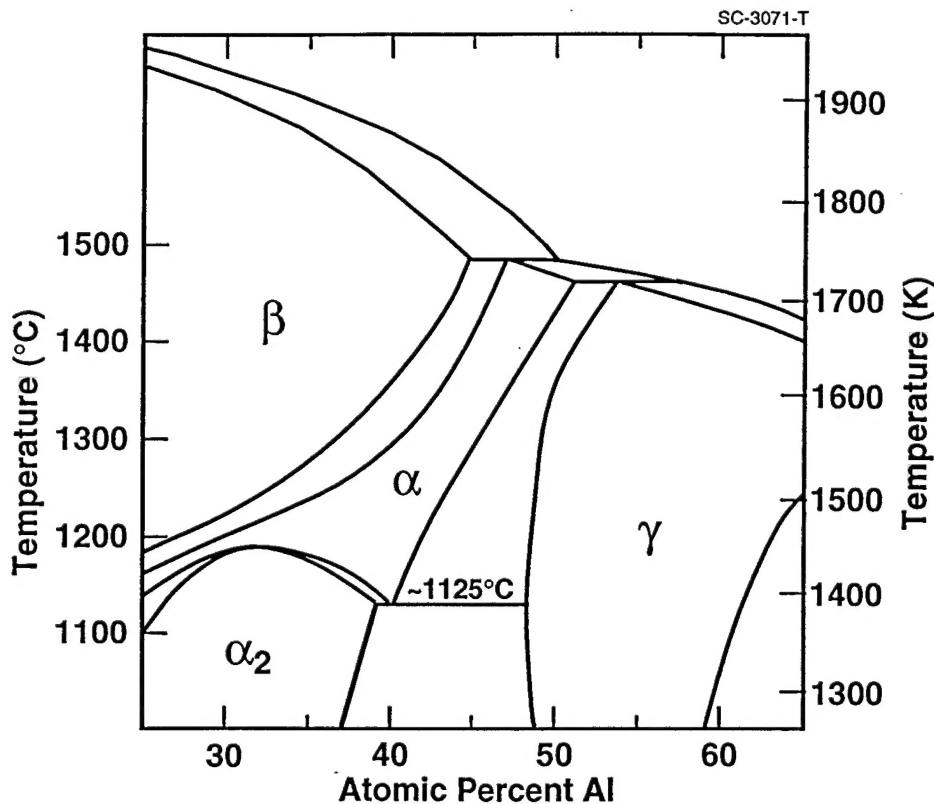


Figure 1 - TiAl equilibrium phase diagram

In this study, compression workability testing has been coupled with metallographic characterization to investigate the influence of primary ingot breakdown on microstructural refinement and chemical homogeneity. The necessity for an initial homogenization step prior to ingot breakdown was addressed by the testing of as cast and cast + homogenized material. The alloy compositions chosen for this study straddled the peritectic composition: Ti-45at%Al, a hypo-peritectic composition, and Ti-47at%Al, a hyper-peritectic alloy. A hyper-peritectic alloy containing Mo was also selected for this study, as high Al alloys exhibit a greater degree peritectic segregation than their low Al counterparts and the Mo addition will highlight this segregation. Boron was incorporated into all of the alloys, as such additions can retard elevated temperature grain growth (11).

The initial applications of  $\gamma$ TiAl alloys will probably involve as-cast materials. Grain refinement is a critical issue in as-cast components and this is no less true for the titanium aluminides. Very large grains can have a detrimental effect on the strength and the toughness of cast near-gamma alloys. It is well established that boron additions are a very potent inoculant for refining the grain size of cast gamma titanium aluminide alloys (12, 13). Boron additions of at least 0.5at% are required to produce grain refinement in as-cast titanium aluminide alloys (13). Even at such low levels, <1at%, boron additions produce a dispersion of boride particles throughout the microstructure (14-16). In binary alloys, the Ti/Al ratio help to determine the morphology of the boride phase (14-16) while the amount of boron added is the prime determinator of the identity of the boride, TiB or TiB<sub>2</sub> (14, 16). Refractory metal additions can also have an effect; Ta and Nb additions can be incorporated into the borides or lead to the precipitation of TaB or NbB (17, 18).

The control of grain size is also very important in wrought materials including gamma titanium aluminide alloys. Grain size control must be maintained during processing operations and particularly during final heat treatment operations. The most desirable microstructural condition in these alloys remains to be determined, but as the debate about the virtues of duplex versus fully lamellar microstructures continues, it is obvious that the microstructure will ultimately be dictated by the application conditions (19). In certain cases, a fine, fully lamellar colony microstructure will be most advantageous. The addition of low levels of boron to wrought near-gamma alloys has been gaining acceptance, as it has been shown to retard elevated temperature grain growth in the single phase alpha regime (11). There has, however, been some concern about the ability to obtain the "optimum" microstructure in B-stabilized materials.

One part of this study was undertaken in an effort to understand the role of borides during the wrought processing and subsequent heat treatment of near-gamma titanium aluminides. A hyper-peritectic alloy containing Mo was selected for this study; high Al alloys exhibit a greater degree peritectic segregation than their low Al counterparts and the Mo addition highlights this segregation. In addition, the simultaneous addition of Mo and B to near-gamma titanium aluminide alloys has not previously been examined.

## Experimental Method

The objective of this research was to define an optimum path for attaining a uniform fine grain size in the intermetallic alloy  $\gamma$ -TiAl. This task was accomplished by developing an understanding of the microstructural evolution during hot working and subsequent static recrystallization. Hot workability testing allowed the establishment of a quantitative framework for the selection of thermomechanical processing parameters.

### Alloy Composition and Heat Treatment

A 100mm diameter ingot of each composition was produced by Duriron, Dayton, OH. The ingots were prepared using an induction skull melting technique and the melts were poured into graphite molds. The aim and actual compositions are given in Table I.

Table I - Composition of Ingots (at%)

Aim Composition	Al	B	Mo	C	O (wppm)
Ti-47Al-0.2B	48.0	0.18	-	0.03	650
Ti-45Al-0.2B	45.7	0.16	-	0.03	640
Ti-47Al-2Mo-0.2B	47.5	0.21	1.8	0.03	790

A series of heat treatments was performed to determine the microstructural response to homogenization. If there can be said to be an industry standard for the heat treatment of cast  $\gamma$  ingots, it is a HIP cycle of 1260°C for 4 hours. Therefore, heat treatments of 4 hours were carried out at 1250°C and the temperature was increased by 50°C increments until homogenization was achieved. Specimens for heat treatment were wrapped in Ta foil and encapsulated in quartz tubes backfilled with a partial pressure of argon. All heat treatments were finished with an air cool during which the samples remained in their glass capsules.

Based on the results of these experiments, the ingots were homogenized prior to forging; 4 hours at either 1350°C or 1400°C, for the low and high Al alloys respectively. Forging preforms, 150mm tall x 100mm in diameter, were then EDM machined from the ingots. These preforms were forged on the research press at Wyman Gordon, Houston, at 1150°C at an initial strain rate of  $10^{-3}\text{s}^{-1}$ ; the final height was  $\approx 60\text{mm}$  for an average true strain of 0.9.

Post-forging heat treatments were performed to determine the microstructural response. Specimens for heat treatment were wrapped in Ta foil and encapsulated in quartz tubes backfilled with a partial pressure of argon. All heat treatments were finished with an air cool, during which the samples remained in their glass capsules.

## Hot Workability

Specimens for compression testing were electro-discharge-machined (EDM) from 12.5mm thick slices taken from the top of the Duriron ingots or from the forged pancakes. The compression cylinders were  $\approx 7.6$ mm diameter and were removed from a circle having a radius of approximately three quarters of the total ingot or pancake radius. The sequential cutting of the cylinders around the radius of the ingot left a raised vertical line of material down the side of each cylinder; with this line as a reference mark, the orientation of each sample with respect to the radial direction in the ingot could be easily determined. The ends of these right circular cylinders were polished flat and perpendicular to the cylinder axis. Hot compression testing was carried out in a Centorr furnace mounted on an Instron test machine. All testing was conducted in a vacuum of  $5 \times 10^{-3}$  Pa or better. The compression platens were silicon nitride backed with W rams and the specimens were lubricated with boron nitride to reduce frictional effects. The silicon nitride platens were not deformed by the testing procedure. Extensometry, using LVDT sensors attached to the W rams, was used to record the displacement. Both the load and the extension were recorded digitally. Temperature was recorded by a thermocouple placed near the compression specimen.

## Microstructural Characterization

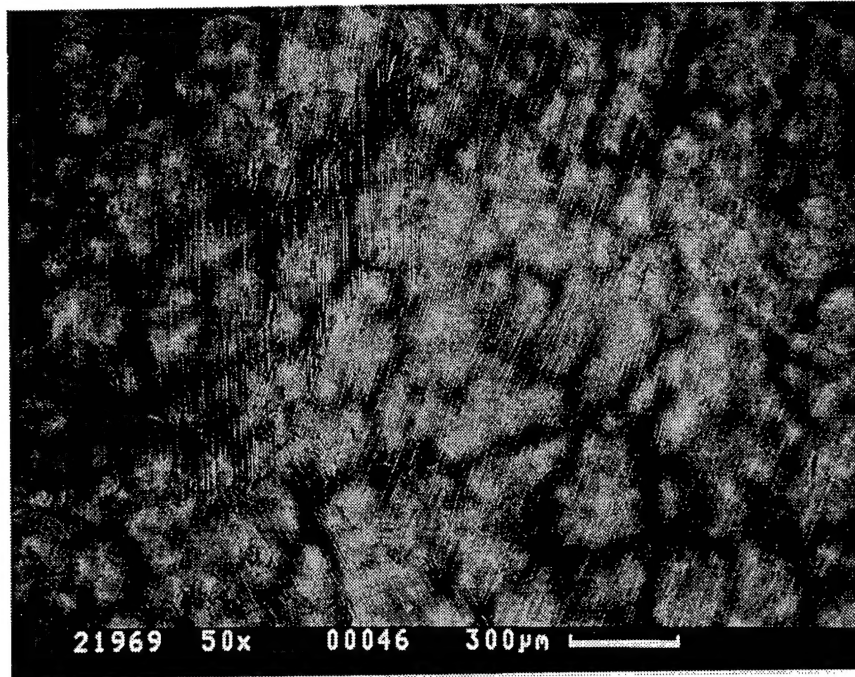
The principal microstructural characterization method used was backscatter image SEM on unetched electropolished surfaces. This method provides both chemical and microstructural information as the image is formed through a combination of atomic number (Z) contrast and orientation due to electron channeling.

All TEM observations were performed on a Philips CM30 operated at 300kV. TEM observations were carried out in the as-cast condition, after 60% forging at 1150°C and after forging + heat treatment (1380°C for 2 hours followed by an air cool). Electron transparent thin foils were prepared by cutting thin slices either perpendicular or parallel to the forging direction. These slices were then ground to roughly 200 $\mu$ m before the punching out of 3mm discs. Subsequent electropolishing was carried out in an electropolishing unit, using a methanol-4% H<sub>2</sub>SO<sub>4</sub> electrolyte at -10°C at a current of 95mA. All electron negatives were digitized at 600dpi on a flatbed scanner with transparency attachment. Image processing was carried out with Adobe photoshop prior to final printing.

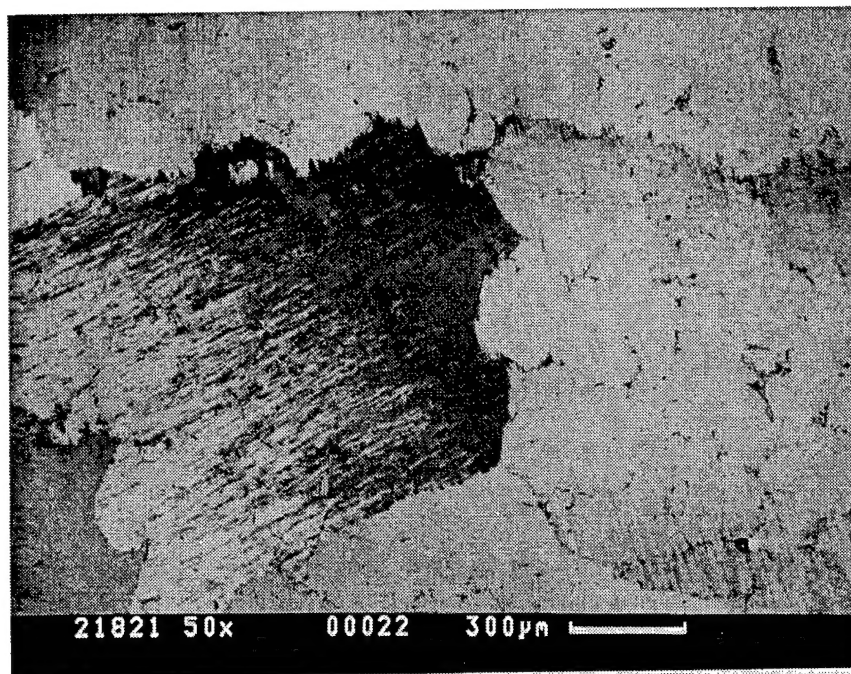
## **Results**

### **Cast and Homogenized Microstructures**

Ti-45.7Al-0.2B The microstructure of the hypo-peritectic alloy in the cast condition and following homogenization heat treatment is shown in Figure 2. In the as-cast condition, the alloy is fully lamellar, as shown in Figure 2a, and backscatter contrast in the SEM reveals little compositional segregation. The Ti-Al phase diagram, shown in Figure 1, indicates that during solidification, the first material to solidify would be a low Al  $\beta$  ( $\approx 40$ at%Al) but that solidification to single phase  $\alpha$  of the peritectic composition of



(a)



(b)

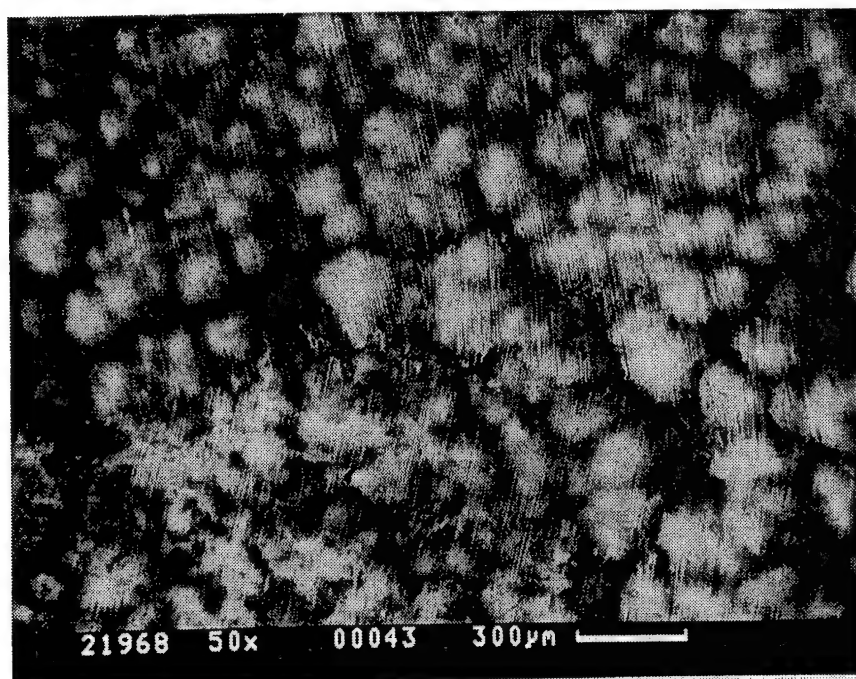
Figure 2 - Microstructure of Ti-45.7Al-0.2B:  
(a) as cast and (b) after an homogenization heat treatment at 1350°C for 4 hours.



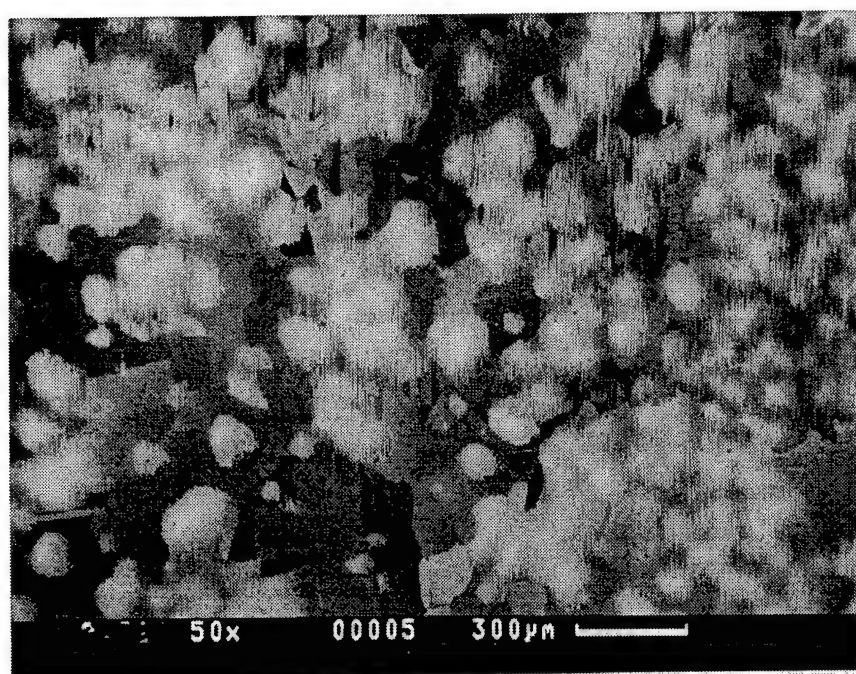
The Ti-Al phase diagram, shown in Figure 1, indicates that during solidification, the first material to solidify would be a low Al  $\beta$  ( $\approx 40\text{at}\%\text{Al}$ ) but that solidification to single phase  $\alpha$  of the peritectic composition of  $46.5\text{at}\%\text{Al}$  will intervene before significant coring of the dendrites occurs. The maximum composition difference between dendrite core and the interdendritic region is thus  $\approx 6\text{at}\%$ ; this small gradient in composition would be largely smoothed out during the residence time in the single phase  $\alpha$  region as the ingot cools. On cooling below  $1325^\circ\text{C}$ , the single phase  $\alpha$  will transform to lamellae of  $\alpha + \gamma$ .

Heat treatment at  $1250^\circ\text{C}$  and  $1300^\circ\text{C}$  had little effect on either the microstructure or the segregation pattern revealed by the backscatter contrast. However, heat treatment at  $1350^\circ\text{C}$  removes all trace of the casting segregation as shown in Figure 2b. At this temperature, the alloy was in the single phase  $\alpha$  region as revealed by the finer lamellar spacing compared with the cast material, a result of air cooling of a small specimen. The locations of former interdendritic regions are identified by the stable boride particles; this is particularly easy to see in the large grain on the right-hand side of Figure 2b.

**Ti-48.0Al-0.2B** The microstructure of the hyper-peritectic alloy in the cast condition and following homogenization heat treatment is shown in Figure 3. During casting of this alloy, the first material to solidify will be  $\beta$  at  $42\text{at}\%\text{Al}$ . The liquid will continue to be enriched with Al until the last liquid to solidify will contain  $\approx 50\text{at}\%\text{Al}$ . The maximum difference in composition between dendrite core and the interdendritic region is greater than for the hypo-peritectic alloy and, in addition, the material must cool through a two phase region. The dendrite cores will transform to  $\alpha$ , but the high Al interdendritic regions transform to single phase  $\gamma$  which will impede compositional rearrangements. Diffusion will have to take place through ordered  $\gamma$  rather than through disordered  $\alpha$ . The cast microstructure, Figure 3a, reflects this solidification sequence; the Ti-rich regions are fully lamellar while the interdendritic Al-rich areas are equiaxed  $\gamma$ . Following heat treatment at  $1250^\circ\text{C}$ , Figure 3b, the microstructure contains considerably more equiaxed  $\gamma$ . The Ti-rich dendrite cores remain fully lamellar and appear to decrease in volume fraction after this heat treatment. After heat treatment at  $1300^\circ\text{C}$ , the lamellar regions expand while the equiaxed interdendritic regions shrink. At temperature, the lamellar regions will be single phase  $\alpha$ , facilitating diffusional rearrangement within these regions, while the interdendritic regions will remain as ordered  $\gamma$  phase. The major change affecting the  $\gamma$  phase will be dissolution and transition to  $\alpha$  phase at the  $\alpha/\gamma$  boundaries. As a result of this rearrangement, the microstructure after heat treatment at  $1300^\circ\text{C}$  appears virtually identical to that in the as-cast condition. Following heat treatment at  $1350^\circ\text{C}$ , the contraction of the equiaxed  $\gamma$  phase has almost reached its conclusion and the microstructure appears more segregated than it was in the cast condition. In the temperature range between  $1350^\circ\text{C}$  and  $1400^\circ\text{C}$ , the alloy becomes single phase  $\alpha$ . During heat treatment at  $1400^\circ\text{C}$ , segregation dissipates and the air cooled microstructure is almost fully lamellar but with some isolated regions of equiaxed  $\gamma$  phase. Once again, locations of former interdendritic regions are revealed by the stable boride particles.



(a)



(b)

Figure 3 - Microstructure of Ti-48.0Al-0.2B: (a) as cast and (b) following heat treatment for four hours at 1250°C.

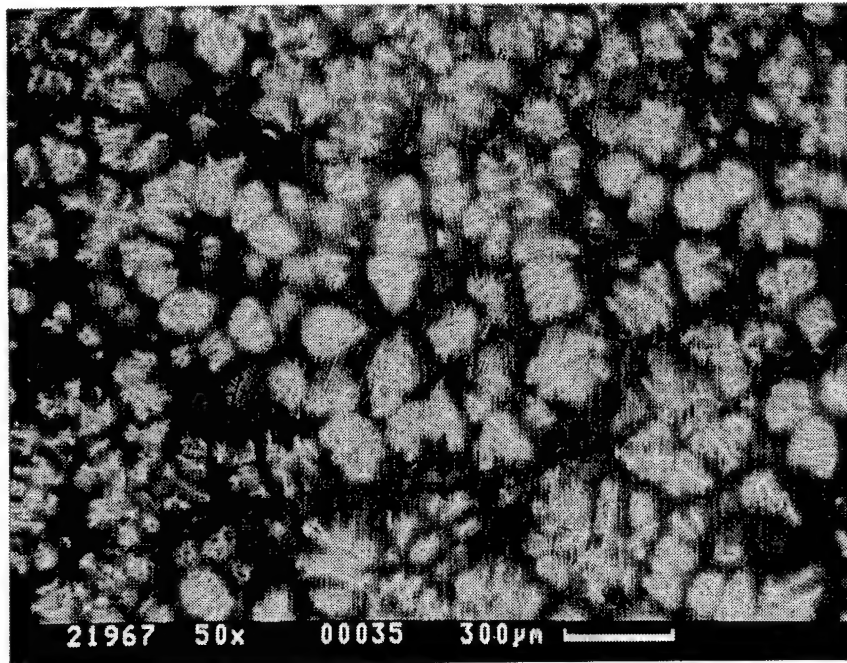


Ti-47.5Al-2Mo-0.2B The binary phase diagram in Figure 1 shows that during casting of this alloy, the first material to solidify will be a  $\beta$  phase that contains 42at%Al. By implication this would be expected to be very rich in Mo. The liquid will continue to be enriched with Al and depleted in Mo until the last liquid to solidify will contain  $\approx 50$  at%Al. As the alloy cools through the two phase  $\alpha+\gamma$  phase field, the dendrite cores, being rich in Mo and low in Al, remain as  $\beta$  phase. The low mobility of the refractory element ensures that the  $\beta$  phase will be retained at room temperature. The surrounding low Al regions transform to disordered  $\alpha$  but the high Al interdendritic regions probably transform to ordered  $\gamma$ . The presence of the ordered  $\gamma$  impedes compositional rearrangements as diffusion through it will be slower than through disordered  $\alpha$ . The final microstructure reflects this solidification sequence as shown in Figure 4. The Mo-stabilized  $\beta$  phase can be seen as the bright dendrite core regions in Figure 4a while the interdendritic regions contain equiaxed  $\gamma$  phase. A higher magnification view, Figure 4b, shows the intradendrite boride phase.

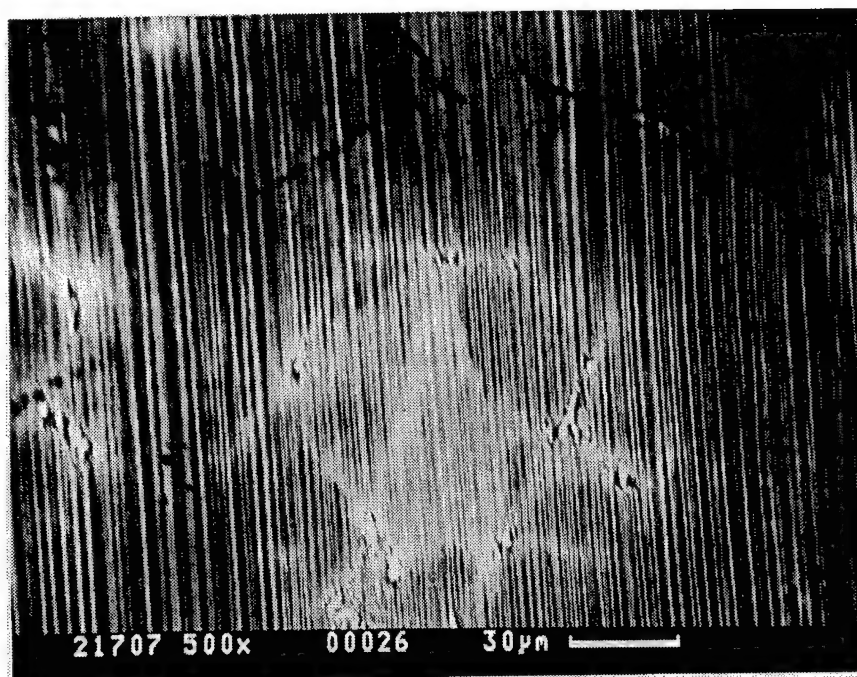
The microstructures resulting from heat treatment of the alloy at a series of temperatures ranging from 1250°C up to 1400°C, are shown in Figure 5. Compared to the as-cast material, the sample heat treated at 1250°C contains considerably more equiaxed  $\gamma$ . These  $\gamma$  grains develop in the Al-rich interdendritic regions. Time at temperatures above 1250°C causes the Ti-rich lamellar regions to expand and the equiaxed interdendritic regions to shrink. At the heat treatment temperature, the lamellar regions will be single phase  $\alpha$ , facilitating diffusional rearrangement within these regions while the interdendritic regions will remain as ordered  $\gamma$  phase. The major change affecting the  $\gamma$  phase will occur at the  $\alpha+\gamma$  boundaries with dissolution and transition to the  $\alpha$  phase. Following heat treatment at 1350°C, this process has almost reached its conclusion; the Al-rich interdendritic  $\gamma$  phase has contracted so much that the microstructure appears more segregated than it was at the beginning of this process, Figure 5b. The continued existence of the interdendritic  $\gamma$  regions impedes homogenization, which is not complete until the  $\alpha$  transus is exceeded; this occurs in the range 1350°-1400°C.

Dispersion of the Mo and elimination of the  $\beta$  phase is the most dramatic effect depicted in this series of micrographs. The  $\beta$  phase, present in the dendrite core regions, remains virtually unaffected by heat treatment at 1250°C and 1300°C: it is seen as the bright, lacy phase in Figures 5a and 5b. After 4 hours at 1350°C, the bright lacy phase is no longer present indicating that the Mo has dispersed sufficiently to allow the  $\beta$  phase to be taken into solution in the disordered  $\alpha$  phase. However, the Mo segregation has not been completely eliminated at 1350°C, Figure 5c. Even after 4 hours at 1400°C, a remnant of Z contrast probably due to Mo segregation, is still visible in Figure 5d.

Therefore, both chemical and microstructural homogeneity can be achieved by temperature alone, provided that the material is a disordered single phase at the heat treatment temperature. However, in the cast material, this results in a very coarse  $\alpha$  grain size which transforms on cooling to a very large lamellar colony size. Within the  $\gamma+\alpha_2$  lamellar colonies, the lamellar spacing is very fine due to the fast cooling rate experienced by the small specimens. Both effects are seen in Figure 5d.

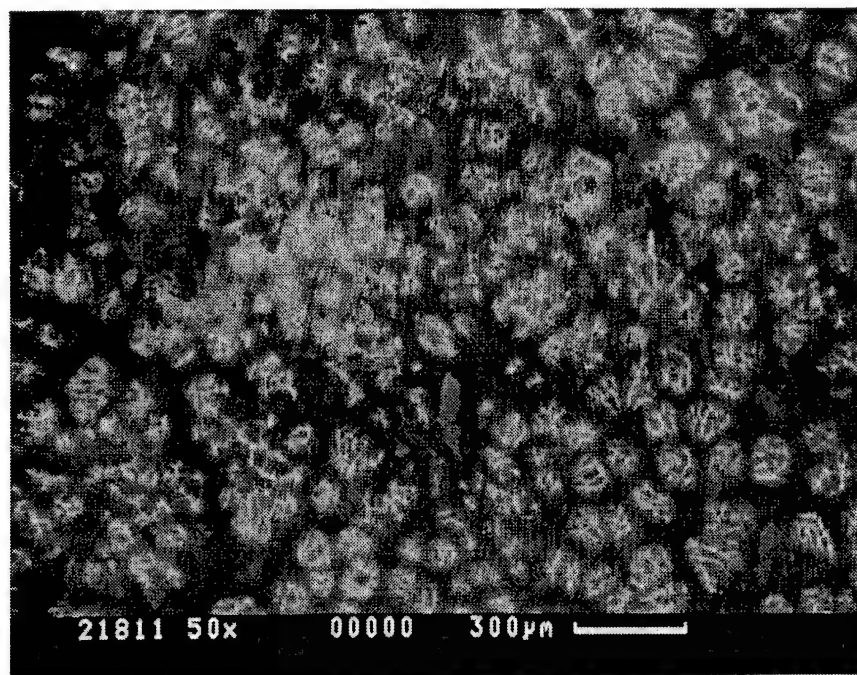


(a)

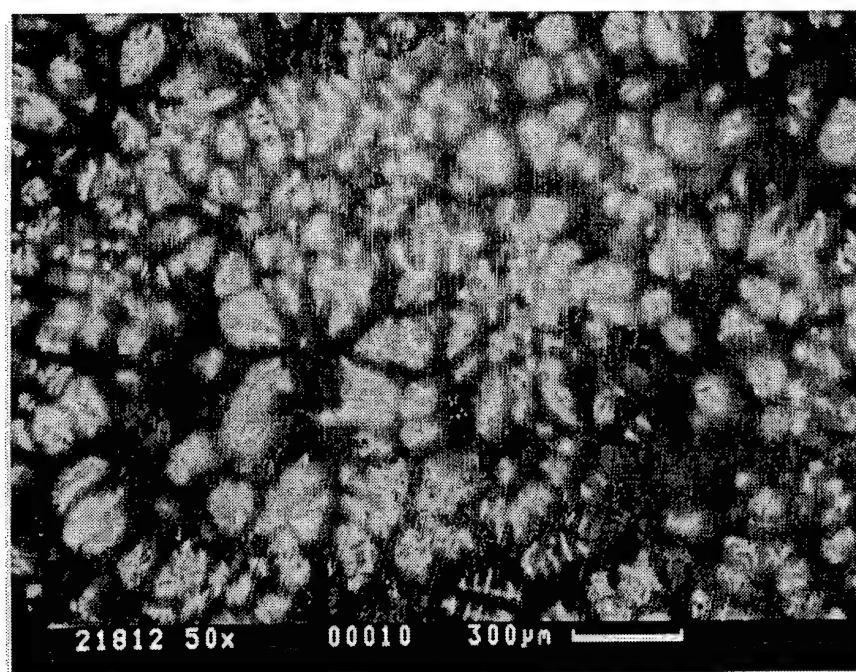


(b)

Figure 4 - As-cast microstructure of Ti-47.5Al-1.8Mo-0.2B as revealed by SEM backscatter imaging

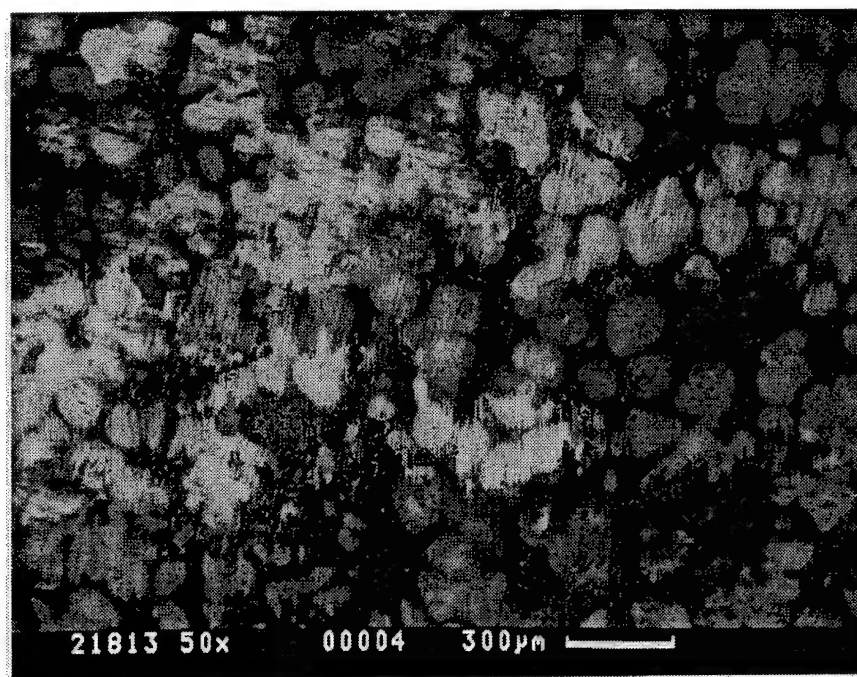


(a) 1250°C

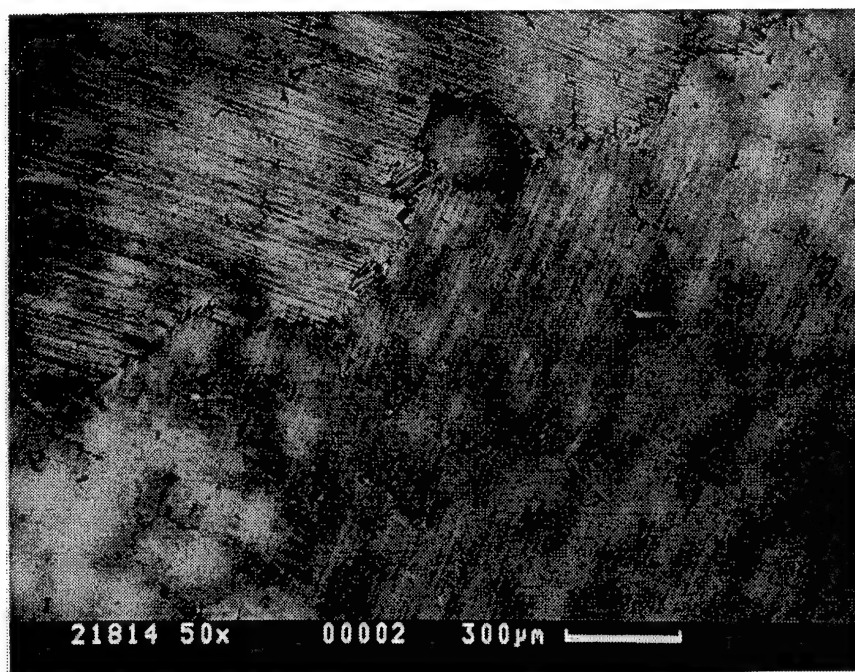


(b) 1300°C

Figure 5 - Microstructural response of Ti-47.5Al-1.8Mo-0.2B to homogenizing heat treatment



(c) 1350°C



(d) 1400°C

Figure 5 - Microstructural response of Ti-47.5Al-1.8Mo-0.2B to homogenizing heat treatment

## Step 1 Hot Workability

The initial workability test parameters were selected to maximize the data relevant for the forging of preforms from the 4" inch diameter ingots. Due to the size of these preforms, forging would necessarily have to be done at a commercial forging house, which placed some limitations on the forging parameters; e.g., a maximum temperature of 1150°C. The test temperatures were 1050°C, 1100°C and 1150°C; all tests were conducted at an initial strain rate of  $10^{-3}\text{s}^{-1}$ . Specimens were tested in each of two microstructural conditions: as-cast and cast+homogenized. The homogenization temperature was that which ameliorated the compositional segregation; i.e. 1350°C for the hypo-peritectic alloy and 1400°C for the hyper-peritectic alloys. Table II presents the data obtained during the hot compression tests. In all cases, the stress-strain curve was characterized by a peak followed by a gradual drop of 40-50% in flow stress to a steady state value.

Table II - Summary of Results from Hot Compression Testing;  $\dot{\epsilon} = 10^{-3}\text{s}^{-1}$

Alloy	Condition	Test temp. (°C)	Peak Stress (MPa)	Total Strain (%)
Ti-46Al-0.2B	as cast	1150	210	50.1
	"	1100	270	49.9
	"	1050	415	49.4
Ti-48Al-0.2B	as cast	1150	214	50.4
	"	1100	248	50.0
	"	1050	314	50.7
Ti-48Al-2Mo-0.2B	as cast	1150	204	50.3
	"	1100	282	50.4
	"	1050	408	49.5
Ti-46Al-0.2B	homogenized	1150	183	50.1
	"	1100	278	49.9
	"	1050	434	49.4
Ti-48Al-0.2B	homogenized	1150	194	50.4
	"	1100	323	50.0
	"	1050	357	50.7
Ti-48Al-2Mo-0.2B	homogenized	1150	189	50.6
	"	1100	310	48.6
	"	1050	429	50.0

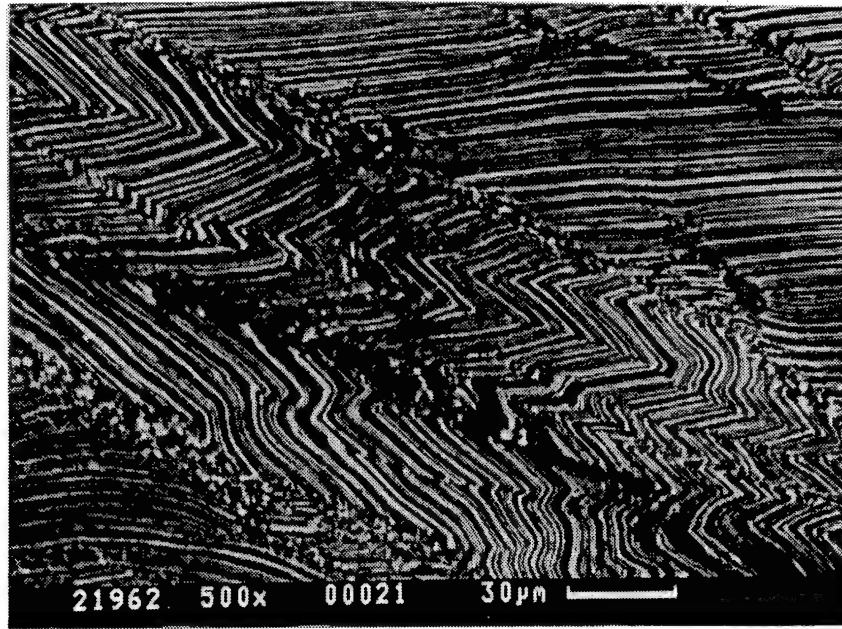


## Microstructures of Step 1 Hot Workability Samples

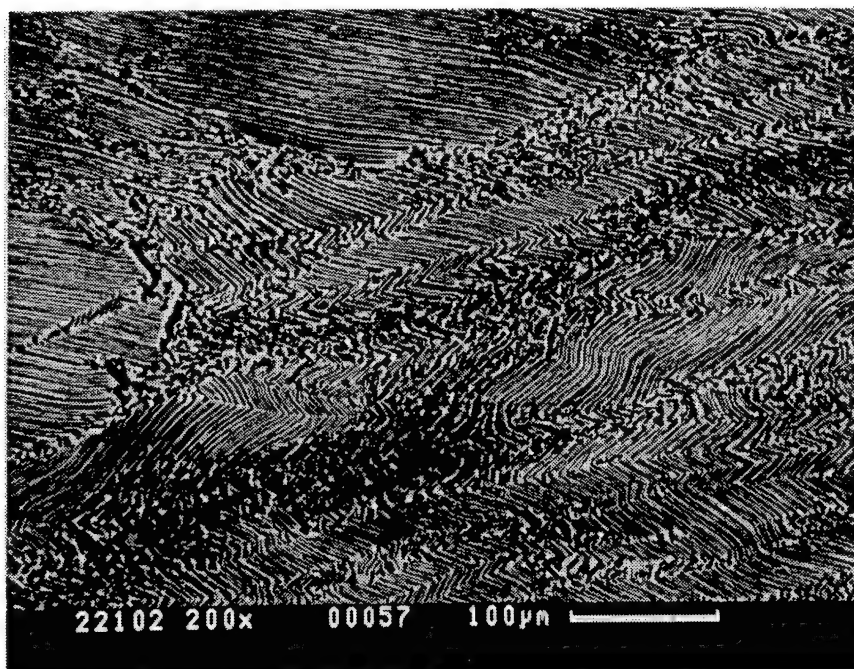
The hot compression data provide some basic information on the stresses necessary to work the material at a given temperature but the most important information is gained by examining the response of the microstructure to the deformation strain. Each alloy exhibited a similar response to deformation at all three temperatures. The only exception to this statement was that wedge cracking was observed at the lowest deformation temperature, 1050°C, particularly in the homogenized, i.e., fully lamellar, microstructures. The following section gives a detailed description and analysis of the results obtained at 1150°C.

Ti-45.7Al-0.2B After compression at 1150°C, the cast lamellar microstructure is traversed by intense shear bands. Figure 6a shows that thin bands of very fine equiaxed grains have formed along these shear bands. Heat treatment at 1200°C for 2 hours yields the microstructure shown in Figure 6b. The bent lamellae caused by passage of the shear bands during compressive deformation are retained in the heat treated microstructure.

Compressive deformation of the homogenized material resulted in a similar microstructure, but deformation of the fine lamellae results in more closely-spaced shear bands, and thicker bands of fine equiaxed grains, Figure 7a. The equiaxed grains were most probably formed by dynamic recrystallization of the heavily worked material in the shear bands. When this material is heat treated at 1200°C the lamellar regions are still retained but the influence of the deformation strain on the lamellar colonies is highlighted by the variation in backscatter contrast within individual lamellar colonies. This variation in contrast is not due to a change in Z, but to a change in orientation, most probably due to deformation-induced lattice rotation of the lamellar colony. The equiaxed  $\gamma$  grains formed by dynamic recrystallization have grown and the  $\alpha$  phase has precipitated from the  $\gamma$  phase in the form of plates parallel to the 4 close-packed 111 planes of the  $\gamma$  phase.

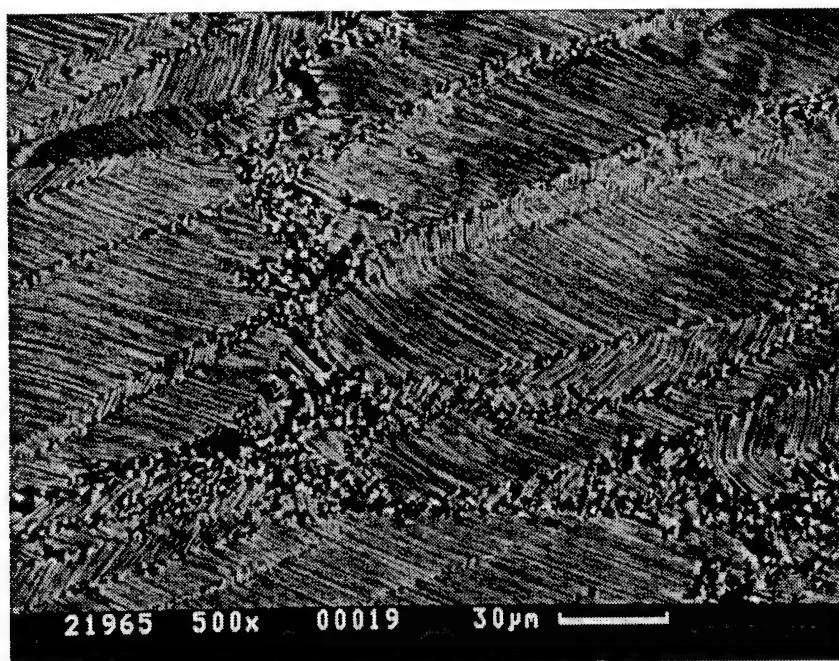


(a)

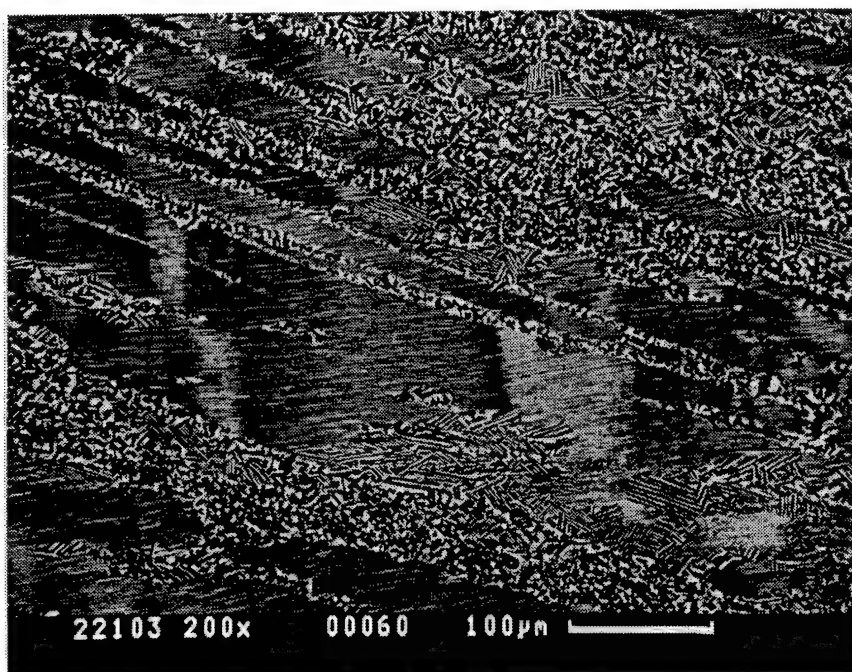


(b)

Figure 6 - Microstructure of cast Ti-45.7Al-0.2B: (a) after 50% strain at 1150°C and (b) following a post deformation heat treatment at 1200°C for 2 hours.



(a)

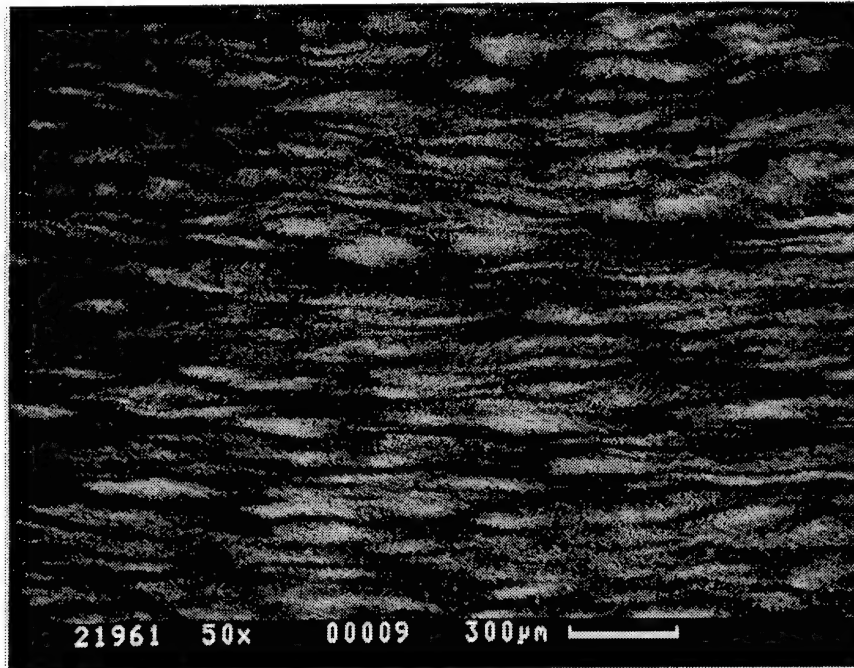


(b)

Figure 7 - Microstructure of homogenized Ti-45.7Al-0.2B: (a) after 50% strain at 1150°C and (b) following a post deformation heat treatment at 1200°C for 2 hours.

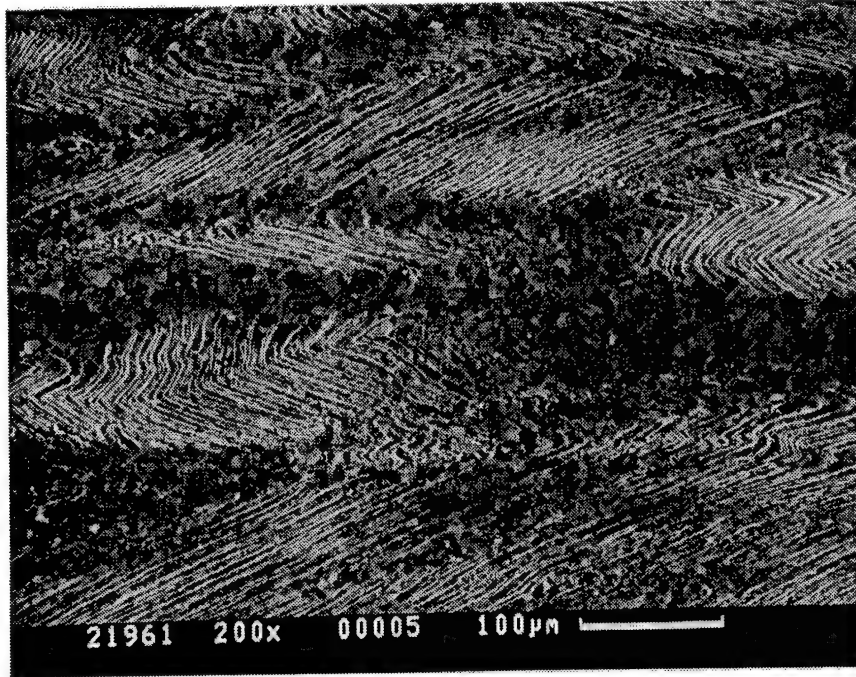


Ti-48.0Al-0.2B As would be expected from the heat treatment study, deformation of the highly segregated hyperperitectic alloy at 1150°C results in little diffusional rearrangement. The high Z regions that were the dendritic cores have merely been elongated perpendicular to the deformation direction, as shown in Figure 8a; the compression axis was vertical. At higher magnifications, the “banded” nature of the deformed microstructure can be easily seen, Figure 8b. Heat treatment at 1200°C leads to grain growth in the equiaxed  $\gamma$  regions but the microstructure remains banded.



(a)

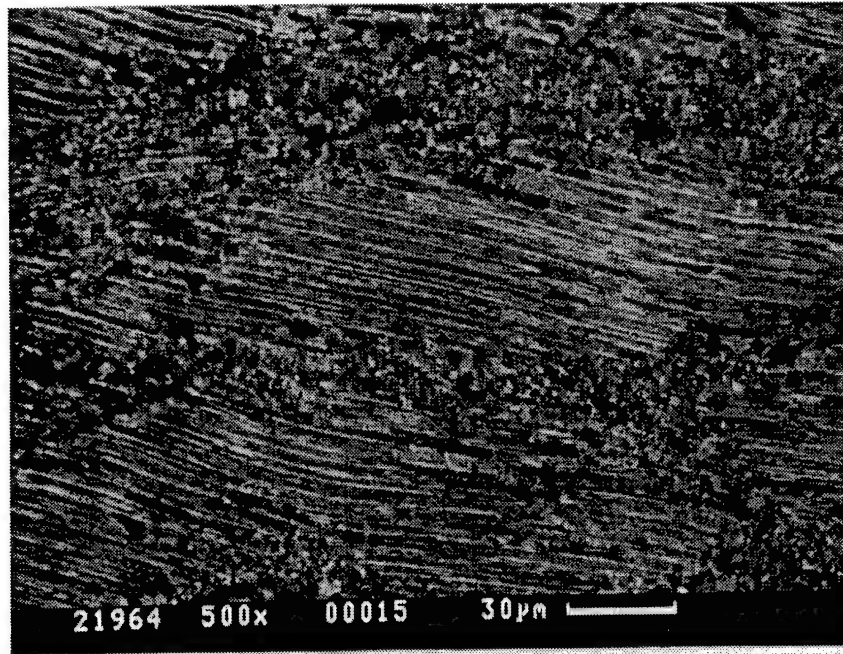
Figure 8 - Deformed microstructure of cast Ti-48.0Al-0.2B.



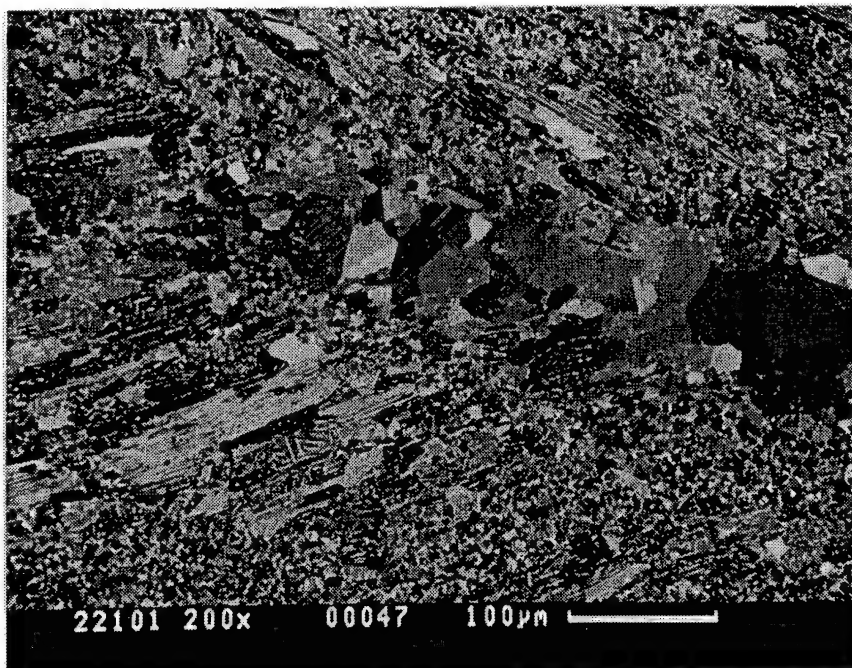
(b)

Figure 8 - Deformed microstructure of cast Ti-48.0Al-0.2B.

Deformation of the fully lamellar, homogenized material yields the microstructure shown in Figure 9a. The microstructure consists of islands of lamellar colonies surrounded by regions of fine, equiaxed, dynamically recrystallized grains. Heat treatment at 1200°C for 2 hours yields the microstructure shown in Figure 9b. The  $\alpha_2/\gamma$  lamellar regions have begun to break-up and spheroidize while grain growth has occurred in regions of  $\alpha_2$ -free, equiaxed  $\gamma$  grains.



(a)



(b)

Figure 9 - Deformed microstructure of homogenized Ti-48.0Al-0.2B:  
(a) as deformed and (b) after 2 hours at 1200°C

Ti-47.5Al-2Mo-0.2B : Figure 10 illustrates the microstructural response of the as-cast material to  $\approx 50\%$  compression at  $1150^{\circ}\text{C}$  and an initial strain rate of  $10^{-3}\text{s}^{-1}$ . As would be expected from the heat treatment study, there has been little diffusional rearrangement of the segregation generated during peritectic solidification at this low temperature. The high Z regions that were the dendritic cores have merely been elongated perpendicular to the deformation direction, Figure 10a. Figure 10b illustrates the “banded” nature of the deformed microstructure. The low Z regions consist of equiaxed  $\gamma$  grains, while the high Z regions retain their lamellar,  $\gamma+\alpha_2$ , nature. Closer examination reveals that some of the lamellae have begun to break up. The hot deformation process has not removed the chemical/microstructural segregation but has reduced the diffusional distances necessary for subsequent homogenization.

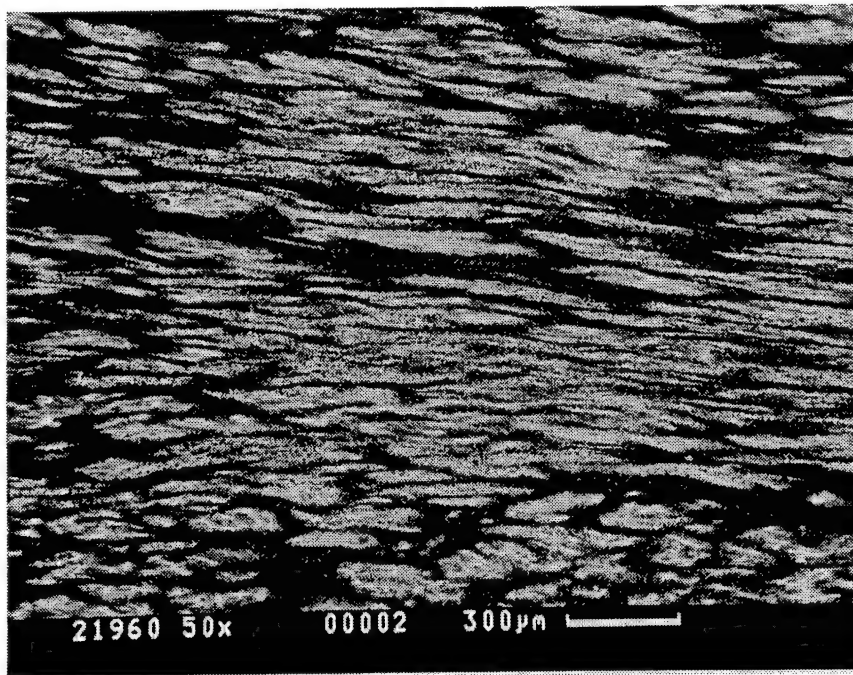
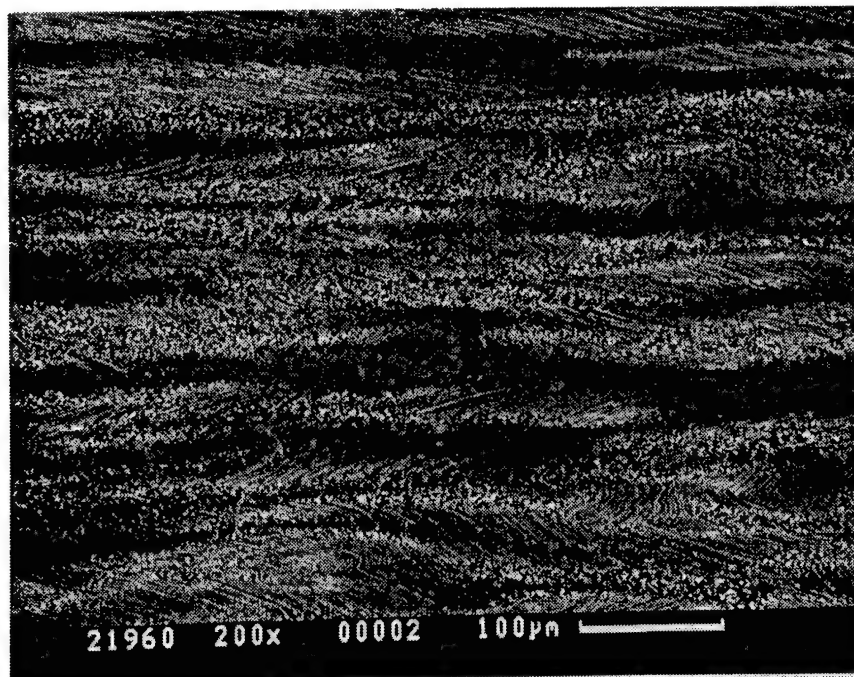


Figure 10: Response to hot deformation of as-cast Ti-47.5Al-1.8Mo-0.2B



(b)

Figure 10: Response to hot deformation of as-cast Ti-47.5Al-1.8Mo-0.2B

Heat treatment of this deformed material at 1200°C for 2 hours yields the microstructure shown in Figure 11. The segregation is little changed from that of the as-deformed material. There has been growth of the equiaxed  $\gamma$  grains but the underlying chemical inhomogeneity leads to the retention of an inhomogeneous microstructure. Higher temperature heat treatments, possibly even above the  $\alpha$  transus, i.e., >1350°C, would be necessary to completely remove the segregation. Exposure to these high temperatures, while removing chemical segregation, will nullify any microstructural refinement effects resulting from the hot deformation.

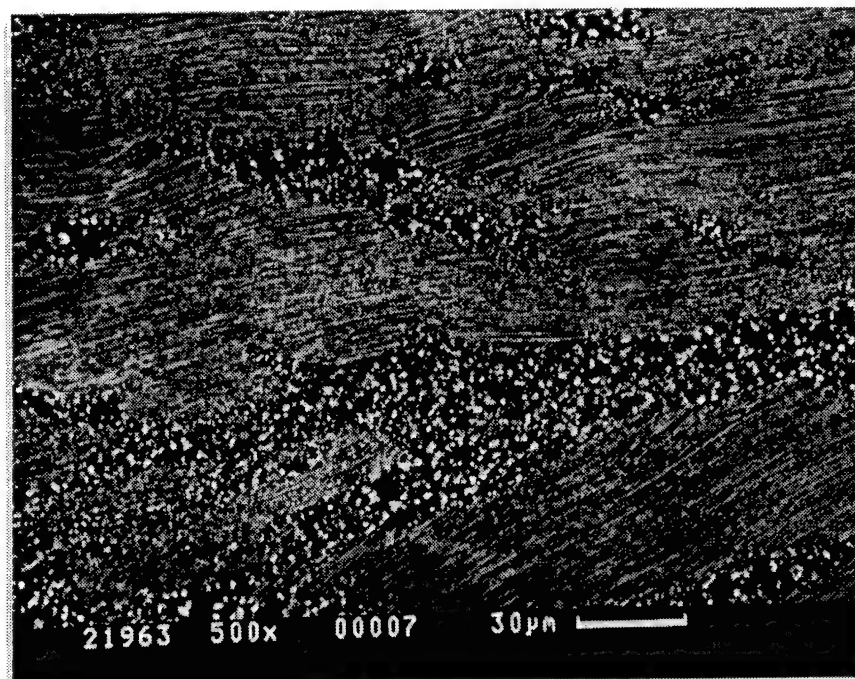
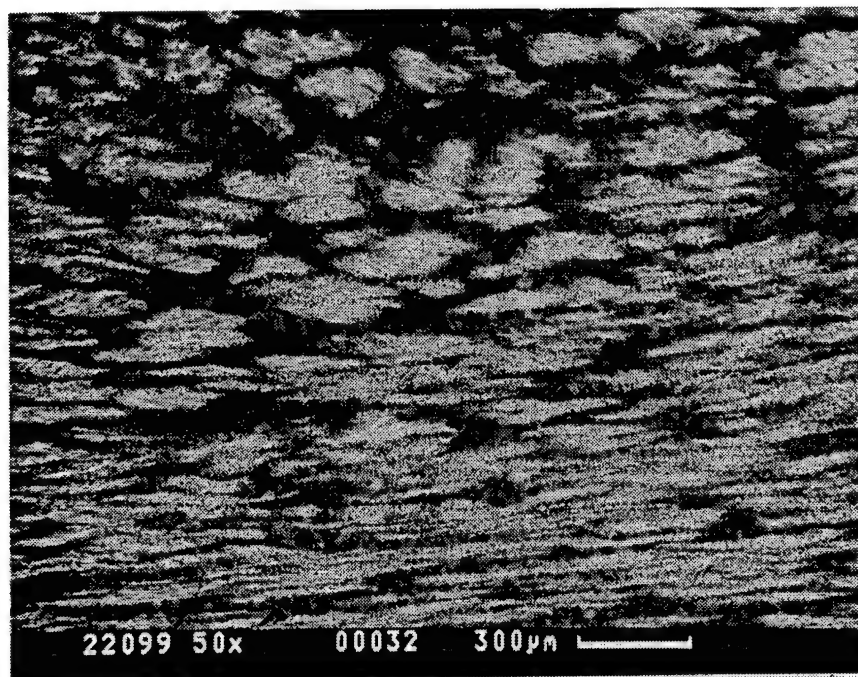


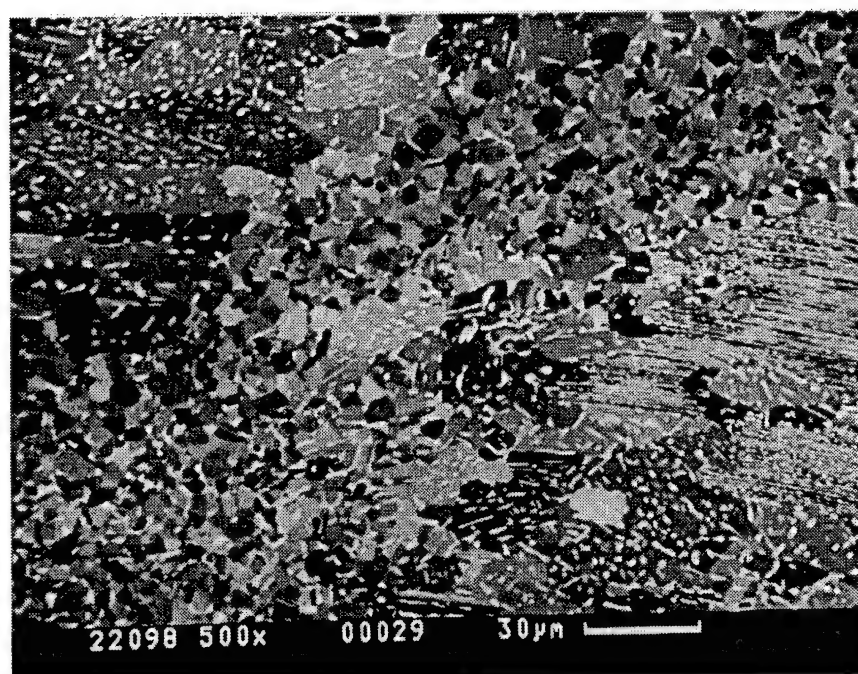
Figure 11 - Response of microstructure in Ti-47.5Al-1.8Mo-0.2B produced by deformation at 1150°C to heat treatment at 1200°C

In the homogenized condition, the microstructure following  $\approx 50\%$  compression at 1150°C consists of islands of lamellar colonies surrounded by regions of very fine, equiaxed, dynamically recrystallized grains as shown in Figure 6a. The lamellae are preferentially oriented perpendicular to the direction of compressive deformation. Their breakup would not be furthered by more deformation in this same direction, but compressive deformation performed in a direction at 90° to the first deformation should lead to compressive "buckling" of these remnant lamellae. Heat treatment of this microstructure at 1200°C yields a bimodal structure with large remnant lamellar colonies surrounded by regions of fine equiaxed  $\gamma$  grains interspersed with  $\alpha_2$  (bright) particles. As shown in Figure 6b, this heat treatment has resulted in significant breakup of the lamellae within the  $\gamma+\alpha_2$  colonies.





(a)



(b)

Figure 12 - (a) The effect of deformation at 1150°C on the homogenized microstructure and (b) the effect of subsequent heat treatment at 1200°C/2 hours.

## Forged Microstructures

Based on the results of these experiments, the ingots were homogenized prior to forging; 4 hours at either 1350°C or 1400°C, for the low and high Al alloys respectively. Forging preforms, 150mm tall x 100mm in diameter, were then EDM machined from the ingots. Following the results of the Step 1 workability experiments, these preforms were forged on the research press at Wyman Gordon, Houston, at 1150°C at an initial strain rate of  $10^{-3}\text{s}^{-1}$ ; the final height was  $\approx 60\text{mm}$  for an average true strain of 0.9.

The macrostructure of a complete longitudinal cross-section through the forging revealed that, as would be expected, the most intensely worked zone was across the central region of the forged pancake, extending out to about half of the radius, Figure 13.

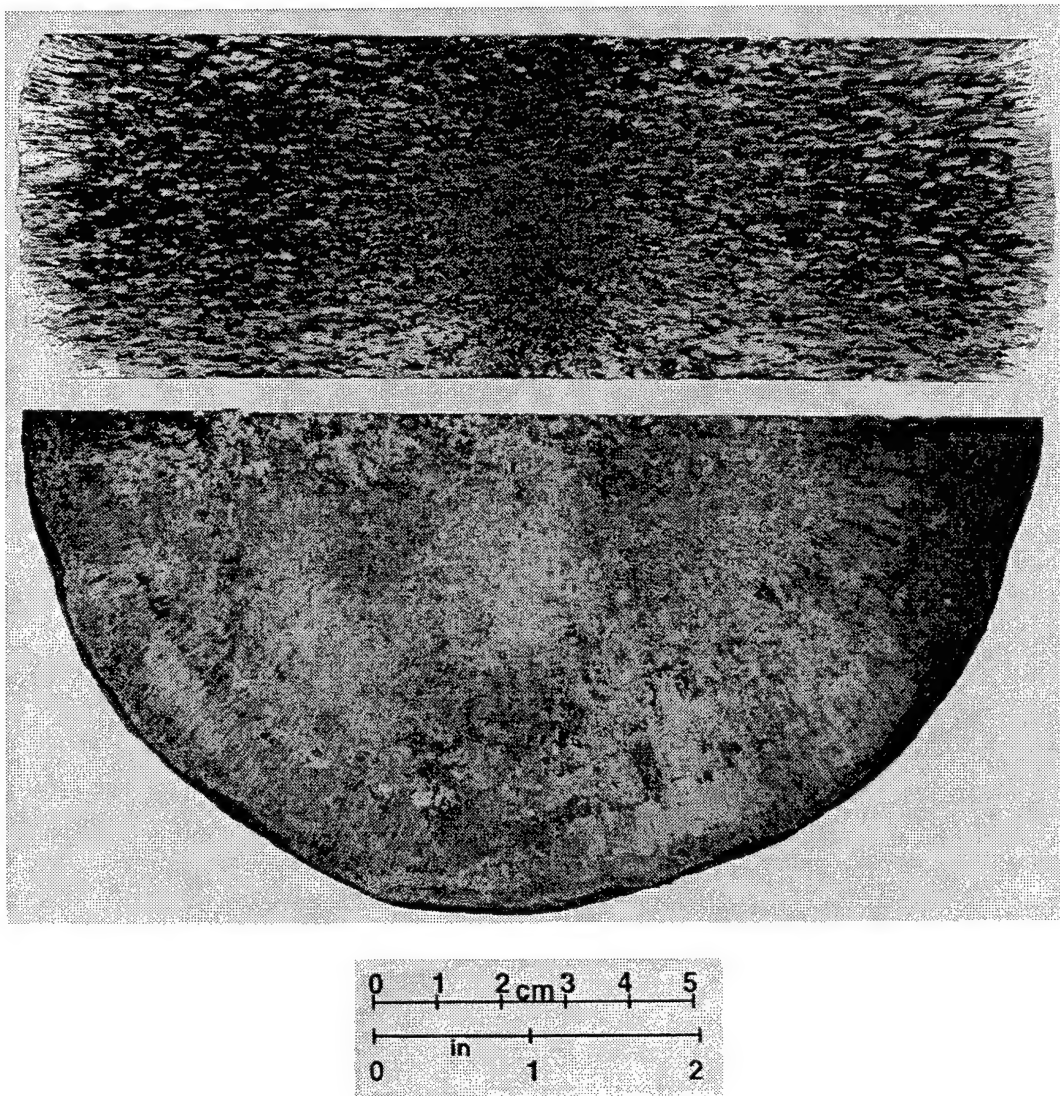


Figure 13: Macrostructure of forging



Microstructures of specimens taken at the half radius position were examined, Figure 14. The Ti-48Al contained large regions of fine equiaxed grains interspersed with regions containing bent lamellae, as shown in Figure 14a. Closer examination of the lamellar regions revealed that the gamma phase had assumed a fine equiaxed structure with a grain size approximating the interlamellar spacing, while the thinner bands of  $\alpha_2$  phase had also begun to break up into individual very fine grains, as shown in Figure 14b. The Ti-46Al consisted of lamellae traversed by intense shear bands, Figure 14c. Closer examination, Figure 14d, revealed that thin bands of very fine equiaxed grains have formed along these shear bands, probably through dynamic recrystallization of the heavily worked material in the shear bands.

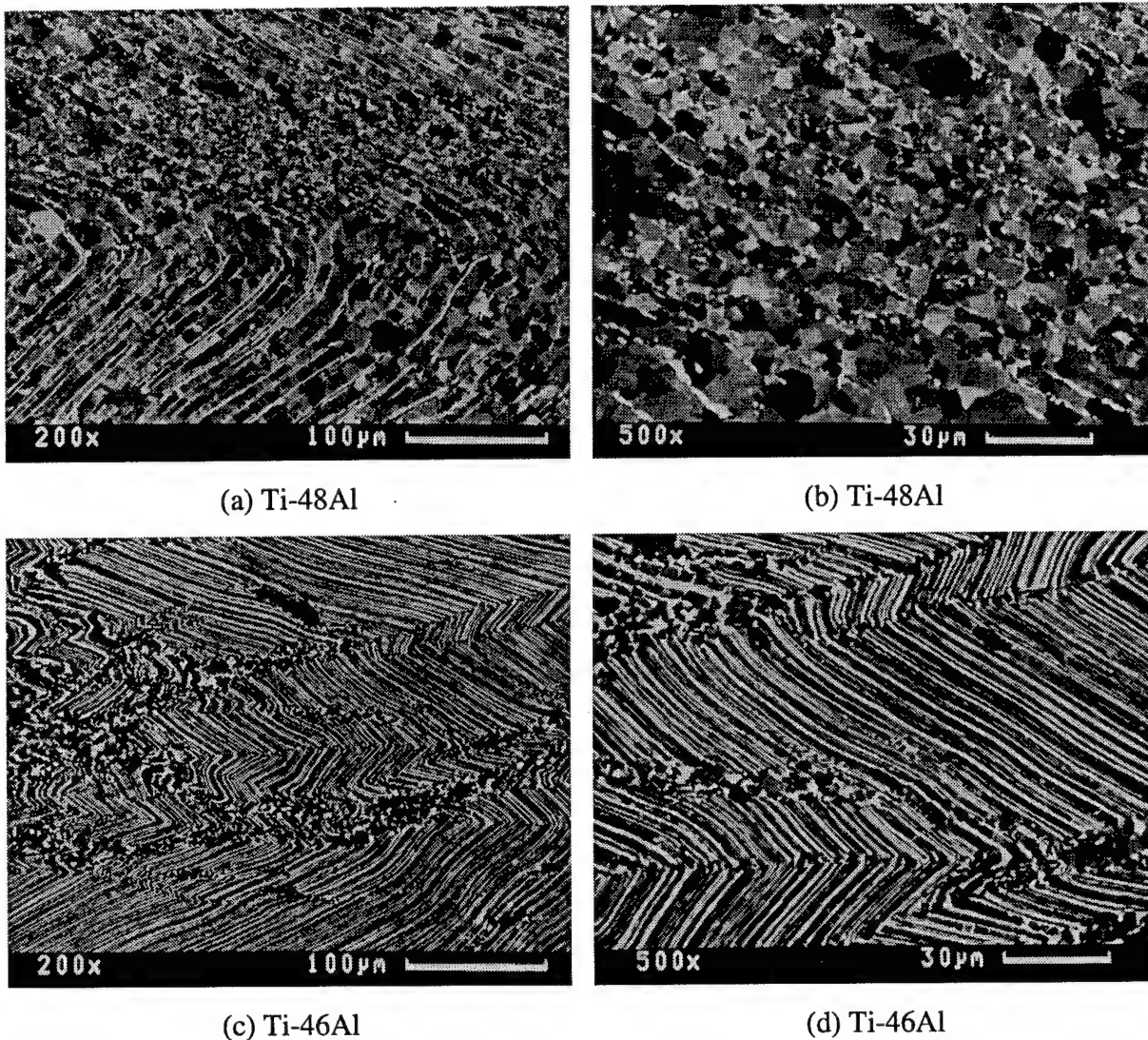
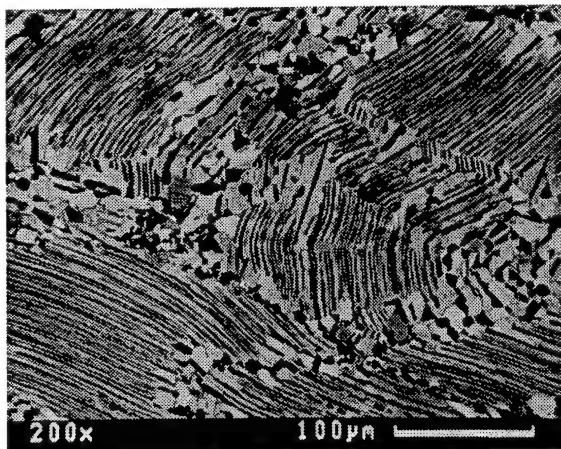


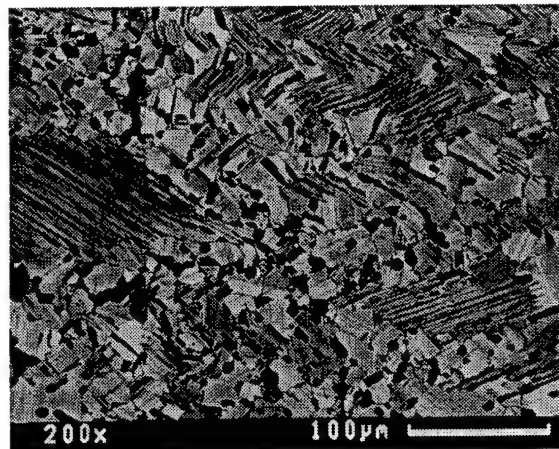
Figure 14: Microstructure of Ti-48Al (a,b) and Ti-46Al (c,d) after forging at  $1150^{\circ}\text{C}/10^{-3}\text{s}^{-1}$  to a strain of 0.9.

## Forged + Annealed Microstructures

The response of the forged microstructures to heat treatment is illustrated in Figures 15 and 16. Heat treatment at temperatures up to 1200°C did not produce any significant changes in the microstructure. Raising the heat treatment temperature to 1300°C results in the microstructures shown in Figure 15a and 16a. Coarsening of the both the lamellar and the equiaxed microstructural units has occurred but they have retained their identities. Longer times at temperature would be needed in order accomplish significant microstructural rearrangement. The equiaxed microstructural features in the low aluminum alloy consist of a mixture of  $\gamma$  grains and very fine lamellar grains. This is more obvious after heat treatment at 1320°C, Figure 15b, as the equiaxed fraction has grown rendering the bimodal lamellar structure more obvious. After heat treatment at 1360°C, the Ti-48Al has a duplex microstructure of fine lamellar grains with residual gamma grains at the lamellar colony boundaries, Figure 16b. A fully lamellar microstructure resulted from annealing for 2 hours at 1340°C for Ti-46Al and 1400°C for Ti-48Al. The  $\approx 100\mu\text{m}$  grain size of these lamellar microstructures is significantly finer than that observed in the cast+homogenized materials.



(a) Ti-46Al: 1300°C/2hrs



(b) Ti-46Al: 1320°C/2 hrs

Figure 15: Microstructure following annealing of Ti-46Al:  
(a) at 1300°C/2hrs and (b) at 1320°C/2 hrs.

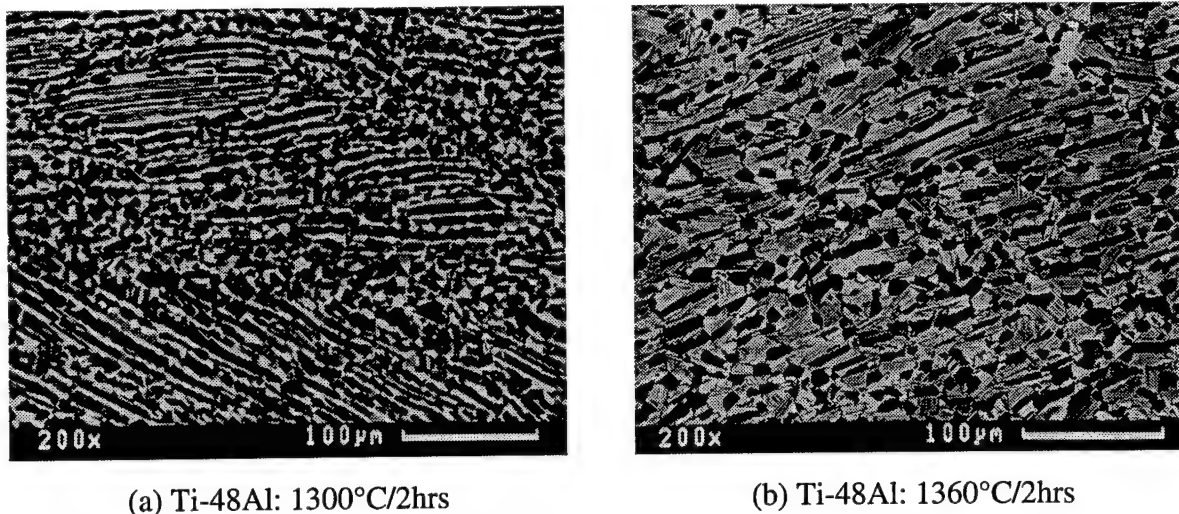
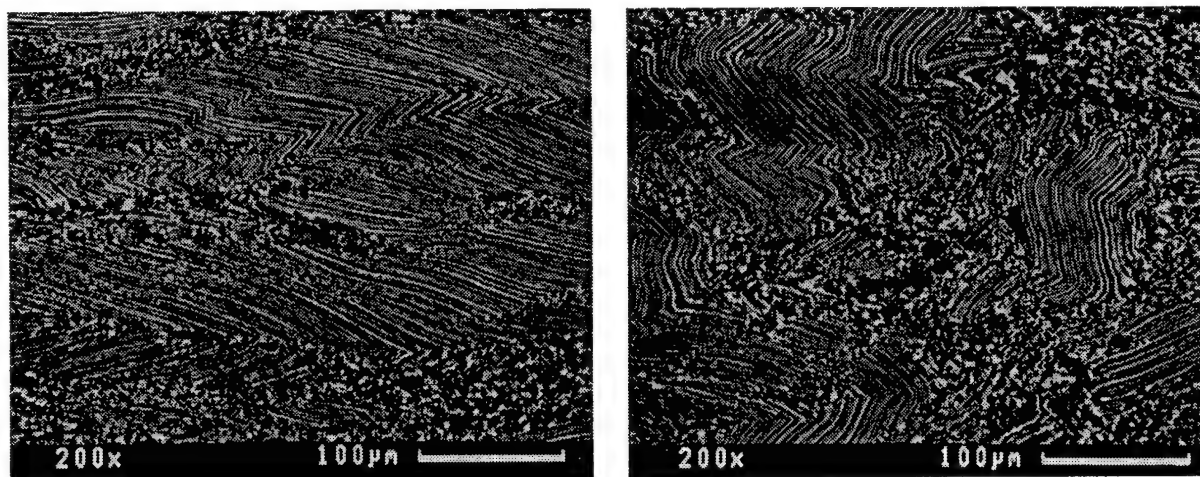


Figure 16: Microstructure following annealing of Ti-48Al;  
(a) at 1300°C/2hrs and (b) at 1360°C/2hrs.

## Step 2 Hot Working Step

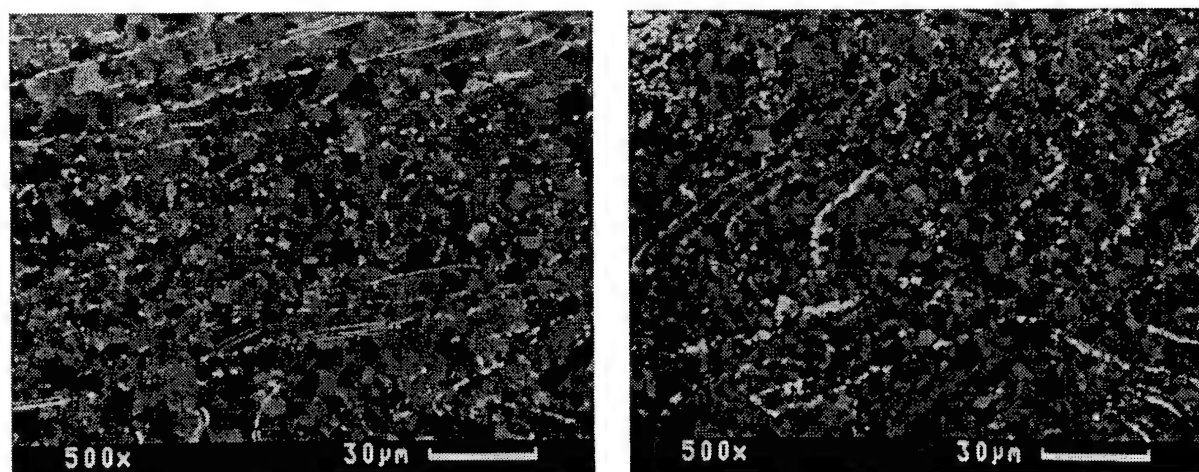
Ti-46Al - without prior annealing: Based on the results of the annealing experiments described above, it was concluded that intermediate annealing would probably not be beneficial to achieving the goal of microstructural homogeneity and refinement in the low Al alloy. Therefore, a series of compression experiments was performed, at an initial strain rate of  $10^{-3}\text{s}^{-1}$ , to determine the optimum temperature for the next forging operation. Specimens were compressed both parallel and perpendicular to the previous forging direction. Figure 17a and 7b show the microstructure after 60% compression at 1100°C. Both microstructures exhibit increased regions of equiaxed grains compared to the forged material, Figure 14c. In the specimen compressed parallel to the prior forging direction, Figure 17a, it can be seen that the lenticular nature of the remnant lamellar colonies that lie perpendicular to the forging direction has become more pronounced. Their elimination is not facilitated when sequential working operations are performed in the same orientation with respect to the microstructural features. When the temperature is raised as high as 1300°C, the equiaxed regions expand but the remnant lamellar colonies remain. However, when the specimen is compressed perpendicular to the prior working operation, deformation of the remnant colonies is enhanced as shown in Figure 17b.



(a) parallel to original forging direction (b) perpendicular to original forging direction

Figure 17: Microstructure of unannealed Ti-46Al following compression at 1150°C;  
(a) parallel and (b) perpendicular to the original forging direction.

Ti-48Al - without prior annealing: To assess the need for an intermediate anneal between hot working operation for Ti-48Al, a series of compression tests at an initial strain rate of  $10^{-3}\text{s}^{-1}$  was performed on this alloy in the as-forged condition. Figure 18 illustrates the results obtained at 1050°C; similar results were obtained at 1100°C and 1150°C. As with the low Al alloy, compression parallel to the prior forging direction resulted in a directional microstructure. In this case the directional feature was undeformed parallel stringers of  $\alpha_2$  in a fine-grained equiaxed matrix, Figure 18a. When the compression is performed perpendicular to the original forging direction, these stringers are deformed and their break-up will be completed with subsequent annealing.



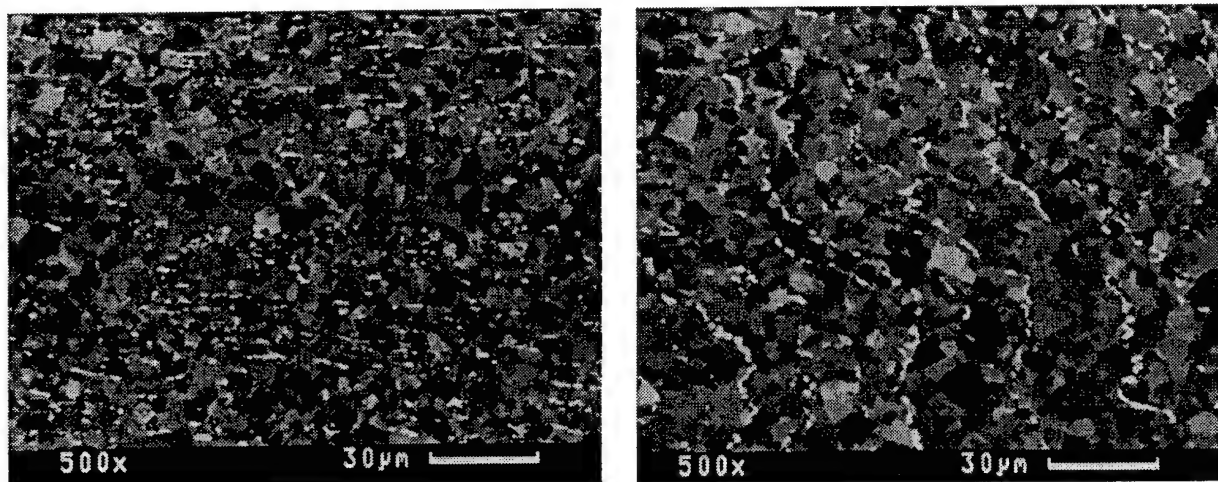
(a) parallel to original forging direction (b) perpendicular to original forging direction

Figure 18: Microstructure of forged Ti-48Al following compression at 1050°C;  
(a) parallel and (b) perpendicular to the original forging direction.



Ti-48Al - with prior annealing: The chosen annealing temperature was 1200°C for 4 hours. A temperature of 1200°C is sufficiently high to facilitate some additional spheroidization of the  $\alpha_2$  phase, but not so high as to allow the formation of islands of disordered  $\alpha_2$  that will transform to lamellar phase on cooling. As before, a series of compression experiments was performed, at an initial strain rate of  $10^{-3}\text{s}^{-1}$ , to determine the optimum temperature for the next forging operation and specimens were compressed both parallel and perpendicular to the previous forging direction. As seen in Figure 19, there appears to be a very minor advantage in terms of break-up of the  $\alpha_2$  phase when the specimens are annealed prior to compression.

Comparing Figures 18 and 19, it can also be seen that there is a refinement of the equiaxed grain size that accompanies hot working at the lower temperature.



(a) parallel to original forging direction      (b) perpendicular to original forging direction

Figure 19: Microstructure of forged+annealed Ti-48Al following compression at 1100°C;  
(a) parallel and (b) perpendicular to the original forging direction.

## Titanium Di-borides in Ti-48Al-2Mo-0.2B

As-cast microstructure: The boride phase is easily seen as dark flakes in the intergranular regions in Figure 4. As illustrated in Figure 5, these boride flakes appear to be unaffected by homogenization heat treatments at temperatures up to 1400°C.

It has been shown that the Ti-borides can assume one of three possible equilibrium crystal structures: (1) orthorhombic TiB ( $B_{27}$ ), (2) body-centered orthorhombic  $Ti_3B_4$  ( $D7_b$ ) or (3) hexagonal  $TiB_2$  ( $C32$ ). In addition, there are several metastable borides including a metastable orthorhombic monoboride  $B_f$ , isomorphous with TaB and a metastable tetragonal boride  $B_g$ , isomorphous with  $\alpha$ -MoB. Complex, fully coherent intergrowths have been shown to occur between  $B_f$ ,  $D7_b$  and  $C32$  and it is not always straightforward to distinguish between these structures solely by means of electron diffraction (16). An example of a complex intergrowth between various boride structures is shown in Figure 20a which shows a boride particle in the as-cast alloy. The corresponding electron diffraction pattern, shown in Figure 20b, indicates that the structure is a mixture of  $C32$ ,  $D7_b$  and  $B_f$ . Detailed identification of the various reflections is shown in Figure 20c.

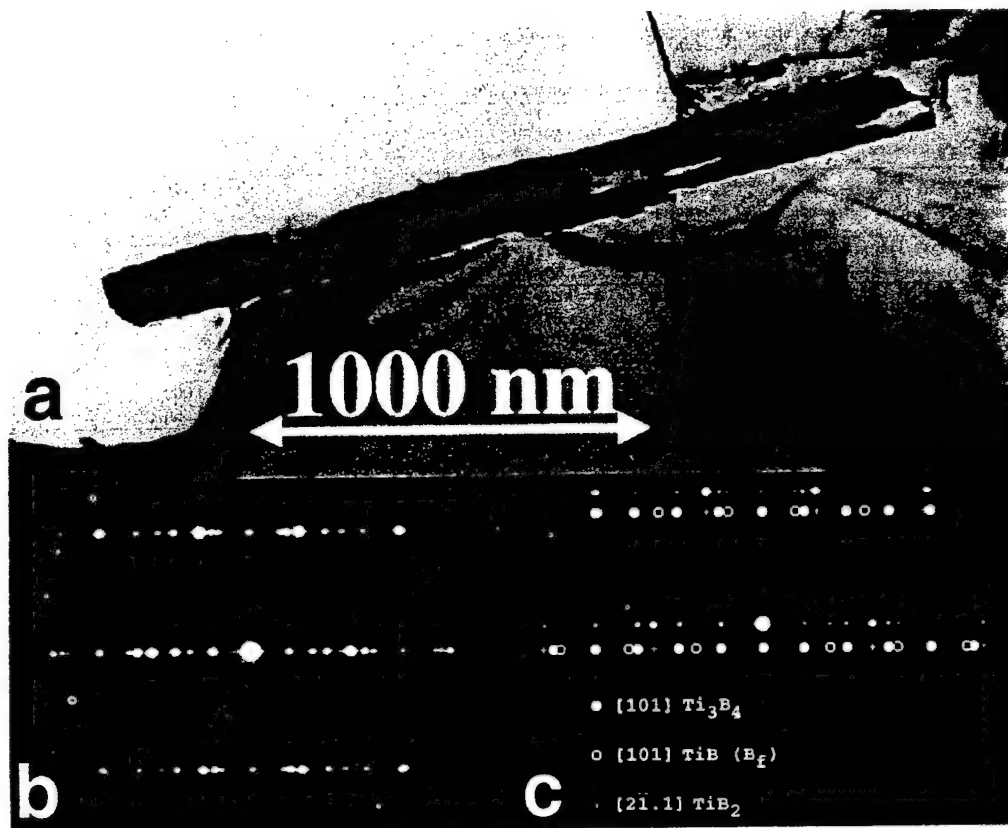


Figure 20: a) Boride flake in the as cast alloy; b) zone axis electron diffraction pattern and c) detailed identification of the diffraction spots.

In many of the boride flakes, a center-line defect was observed indicating that the particle first nucleated as a thin sheet that coarsened into a thicker flake. Depending on the local boron concentration in the melt, a variety of defects, parallel to the center line may form. The observed orientation relations between the borides,  $[101]D_{7b} \parallel [101]B_f \parallel [21.1]C_{32}$ , is as expected. The boride particles were often observed to intersect lamellar colonies at large oblique angles, sometimes perpendicular to the lamellar planes. Although in some cases interfacial dislocations were observed between borides and the surrounding  $\gamma$  plates, a simple orientation between the borides and the surrounding phases could not be found. Particle thickness varied from less than 100nm to about 400nm with aspect ratios as high as 70:1.

**Forged microstructure:** Following forging at 1150°C, the borides flakes had broken up into smaller micron-sized segments. Partial removal of the intergrowth defects indicated that they may have been some boron redistribution. This evolution became more apparent after a 2 hour heat treatment at 1380°C followed by air cooling. The defect density of the boride particles had now decreased to the point where well defined bend contours were observable within them. The boride particles now measured in the micron to submicron range and showed increased faceting, a further sign of boron redistribution. Most boride particles still showed a center-line defect and some were surrounded by  $\gamma$  grains, indicating a residual inhomogeneity in the Al concentration. After the heat treatment step, the microstructure consisted of 80-100 $\mu$ m lamellar colonies; the lamellar spacing was submicron. Colony boundaries were often decorated with  $\gamma$ grains and some large remnant boride flakes could also be observed.

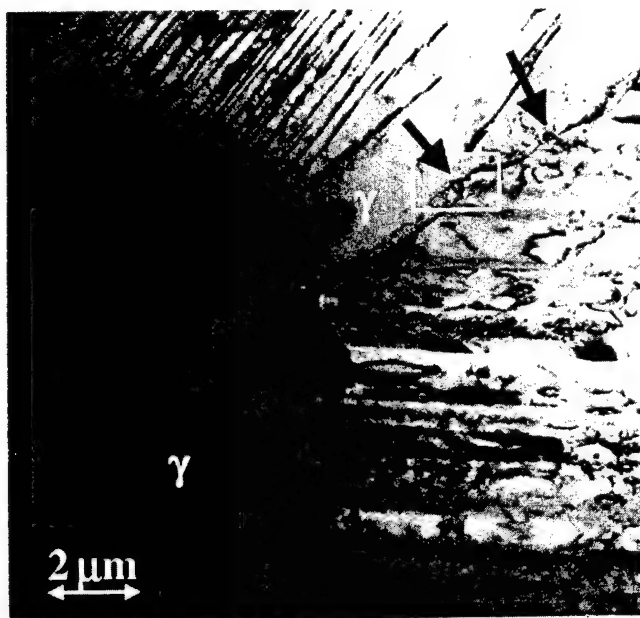


Figure 21: Colony boundary decorated with boride particles in the forged and heat treated alloy. Arrows indicate the location of the borides.

Detailed analysis of the colony boundaries revealed that they are decorated with fine boride particles, 50-100nm long, such as the ones indicated by arrows in Figure 21. Electron diffraction has shown that these fine borides are of the C32 di-boride type. The curvature of the colony boundary close to where they intersect the boride particles suggests that the borides were indeed effective in retarding colony and grain growth.

Preliminary observations using a Gatan Imaging Filter on a JEOL 4000EX HRTEM indicated that there may be boron distributed along the colony boundary. A strong boron electron energy loss signal was observed from the boride particles at the colony boundary and a rather weak signal from the boundary itself.



## Conclusions

The following conclusions can be drawn from examination of the as-cast and the homogenized materials and from the first step workability experiments:

- i) The optimal homogenization heat treatment for the hypo-peritectic alloy, based on dispersion of both chemical and microstructural inhomogeneities, was 1350°C, while the hyper-peritectic alloys, either with or without Mo, required 1400°C.
- ii) An homogenization heat treatment prior to hot working was beneficial for obtaining a more uniform hot worked microstructure.
- iii) The optimal hot working temperature was the highest temperature investigated, 1150°C. Lower temperatures did not show any advantages; the lowest temperature was associated with wedge cracking of the workability samples, particularly in the homogenized material.
- iv) Heat treatment after the hot workability step was beneficial in obtaining a more uniform structure when the starting material was in the homogenized condition.

The following conclusions can be drawn from examining the commercially forged materials and from the Step 2 workability experiments:

- v) Single step hot working of a chemically homogeneous high Al alloy leads to break-up of the initial fully lamellar structure coupled with significant microstructural refinement.
- vi) Single step hot working of a chemically homogeneous low Al alloy results in a highly nonhomogeneous microstructure as the deformation occurs by the formation of intense shear bands and dynamic recrystallization is limited to these highly deformed regions.
- vii) Annealing following forging does not further significantly the goals of microstructural homogeneity and refinement for either Ti-46Al or Ti-48Al.
- viii) For both alloys, hot working perpendicular to the prior forging direction is more successful than hot working parallel to the initial forging direction for achieving the goal of elimination of the remnant lamellar colonies.
- ix) Changing the hot working direction is essential for breaking up the low Al lamellar structure.
- x) Homogenization of the microstructure to a fine-grained equiaxed condition is significantly easier in high Al (hyperperitectic) alloys than in low Al (hypoperitectic) alloys.

- xi) These conclusions for the behavior of high Al alloys versus low Al alloys are also relevant in the context of the highly segregated microstructures possible in modern  $\gamma$ -TiAl alloys.

The following conclusions can be drawn from the examination of the boride constituents in the as-cast and the forged and heat treated material:

- xii) Chemistry fluctuations in the melt during solidification are accommodated by growth of complex, fully coherent intergrowths between the various di-boride structures within the boride flakes.
- xiii) TEM observations provide strong evidence that the borides are effective in retarding grain growth above the  $\alpha$ -transus; the grain boundaries were seen to be pinned quite effectively by boride particles with sizes in the range 50-500nm.
- xiv) Preliminary evidence was also obtained that atomic boron was present along the colony boundaries.

## References

1. Y-W. Kim, "Ordered Intermetallic Alloys Part III: Gamma Titanium Aluminides", Journal of Metals, 46 (7) (1994), 30-39.
2. Y-W. Kim and D.M. Dimiduk, Journal of Metals, Vol. 43, No. 8, 1991, 40-47.
3. C.M. Austin and T.J. Kelly, "Gas Turbine Engine Implementation of Gamma Titanium Aluminide", Superalloys 1996, ed. R.D. Kissinger, D.J. Deye, D.L. Anton, A.D. Cetel, M.V. Nathal, T.M. Pollock and D.A. Woodford, TMS, Warrendale PA, 1996, 539-543.
4. C.M. Austin and T.J. Kelly, Structural Intermetallics, ed. R. Darolia, TMS, Warrendale PA 1993, 21-32.
5. S-C. Huang, Metallurgical Transactions, Vol. 23A, No. 1, 1992, 375-377.
6. S-C. Huang and E.L. Hall, Acta Metallurgica, Vol. 39, No. 6, 1991, 1053-1060.
7. Y-W. Kim, Journal of Metals, Vol. 46, No. 7, 1994, 30-39.
8. P.L. Martin, C.G. Rhodes and P.A. McQuay, "Thermomechanical Processing Effects on Microstructure in Alloys Based on Gamma TiAl", in Structural Intermetallics, edited by R. Darolia et al. (TMS, 1993) 177-186.
9. S.L. Semiatin, "Wrought Processing of Ingot-Metallurgy Gamma TiAl Alloys", in Gamma Titanium Aluminides, edited by Y-W. Kim, R. Wagner and M. Yamaguchi (TMS, 1995) 509-524.
10. P.L. Martin, S.K. Jain and M.A. Stucke, "Microstructure and Mechanical Properties of Wrought Near- $\gamma$  TiAl Alloys", in Gamma Titanium Aluminides, edited by Y-W. Kim, R. Wagner and M. Yamaguchi, (TMS, 1995) 727-736.

11. P.L. Martin and D.A. Hardwick, "Microstructure and Properties of Near- $\gamma$  Alloys Based on Ti-47Al-2Nb-2Cr-1Mo", to be published in Proceedings of the 8th World Conference on Titanium, edited by M. Loretto et al. (Institute of Materials, London, 1996).
12. S-C.Huang and E.L.Hall, "Structures and Properties of Gamma TiAl Alloys Containing interstitial Alloys", High Temperature Ordered Intermetallic Alloys IV, ed. L.A.Johnson, D.P.Pope and J.O.Steigler, Mat. Res. Soc. Proc. 213, Pittsburgh PA, 1991, 827-832.
13. D.E.Larsen, Jr. "Effects of XD TiB<sub>2</sub> Volume Fraction on the Microstructure and Mechanical Properties of a Cast XD Near-gamma Alloy" in Microstructure/Property Relationships in Titanium Aluminides and Alloys, ed. Y-W.Kim and R.R.Boyer, TMS, Warrendale PA 1993, 345-352.
14. M.E.Hyman, C.McCullough, J.J.Valencia, C.G.Levi and R.Mehrabian, Metall. Trans. A 20A, 1847 1989.
15. M.E.Hyman, C.McCullough, C.G.Levi and R.Mehrabian, Metall. Trans. A 22A, 1647 1991.
16. M.De Graef, J.P.A. Lofvander, C.McCullough and C.G.Levi, Acta Metall. Mater. 40 3395, 1992.
17. M.De Graef, J.P.A. Lofvander and C.G.Levi, Acta Metall. Mater. 39 2381, 1991
18. J.J.Valencia, Lofvander, C.McCullough, C.G.Levi and R.Mehrabian, Mat. Sci. Eng. A144, 25 1991.
19. D.M.Dimiduk, "Gamma Titanium - An Emerging Materials Technology", Gamma Titanium Aluminides, ed. Y-W. Kim, R.Wagner and M.Yamaguchi, TMS, Warrendale PA, 1995, 3-20.